

# The wiring diagram of a glomerular olfactory system

Matthew E. Berck<sup>1\*</sup>, Avinash Khandelwal<sup>2\*</sup>, Lindsey Claus<sup>1</sup>, Luis Hernandez-Nunez<sup>1</sup>,  
Guangwei Si<sup>1</sup>, Christopher J. Tabone<sup>1,4</sup>, Feng Li<sup>3</sup>, James W. Truman<sup>3</sup>, Rick D. Fetter<sup>3</sup>,  
Matthieu Louis<sup>2,c</sup>, Aravinthan D.T. Samuel<sup>1,c</sup>, Albert Cardona<sup>3,c</sup>

May 12, 2016

\*: equal contribution.

c: corresponding authors: [cardonaa@janelia.hhmi.org](mailto:cardonaa@janelia.hhmi.org), [adtsamuel@gmail.com](mailto:adtsamuel@gmail.com), [Matthieu.Louis@crg.eu](mailto:Matthieu.Louis@crg.eu)

1: Harvard University, Department of Physics and Center for Brain Science.

2: EMBL-CRG Systems Biology Program, Centre for Genomic Regulation (CRG), The Barcelona Institute of Science and Technology, Dr. Aiguader 88, 08003 Barcelona, Spain; Universitat Pompeu Fabra (UPF), Barcelona, Spain.

3: HHMI Janelia Research Campus, 19700 Helix Dr., Ashburn, VA 20147.

4: Current address: Fly Base.

## Abstract

The sense of smell enables animals to react to long-distance cues according to learned and innate valences. Here, we have mapped with electron microscopy the complete wiring diagram of the *Drosophila* larval antennal lobe, an olfactory neuropil similar to the vertebrate olfactory bulb. We found a canonical circuit with uniglomerular projection neurons (uPNs) relaying gain-controlled ORN activity to the mushroom body and the lateral horn. A second, parallel circuit with multiglomerular projection neurons (mPNs) and hierarchically connected local neurons (LNs) selectively integrates multiple ORN signals already at the first synapse. LN-LN synaptic connections putatively implement a bistable gain control mechanism that either computes odor saliency through panglomerular inhibition, or allows some glomeruli to respond to faint aversive odors in the presence of strong appetitive odors. This complete wiring diagram will support experimental and theoretical studies towards bridging the gap between circuits and behavior.

## Introduction

An animal uses its sense of smell to navigate odor gradients, and to detect the threat or reward associated with an odor. In the nervous system, odorants are detected by olfactory receptor neurons (ORNs) whose axons organize centrally into glomeruli by olfactory receptor type [1, 2]. Uni- and multi-glomerular projection neurons (PNs) relay olfactory inputs to higher-order brain areas [3, 4]. Common between mammals and insects [5, 6], PNs target two major brain centers, one associated with learning and memory (such as the mushroom bodies (MB) in insects), and another that mediates some innate behaviors (such as the lateral horn (LH) in insects) [3, 7–9]. Local neurons (LNs) mediate communication between glomeruli, implementing compu-

tations such as gain control [10]. While the connectivity of a few glomeruli has been recently partially reconstructed in the adult fly [11], the complete number and morphology of cell types and the circuit structure with synaptic resolution is not known for any glomerular olfactory system.

In the *Drosophila* larva, we find a similarly organized glomerular olfactory system of minimal numerical complexity (Figure 1a). In this tractable system, each glomerulus is defined by a single, uniquely identifiable ORN [12, 13], and almost all neurons throughout the nervous system are expected to be uniquely identifiable and stereotyped [14–17]. Some of the olfactory LNs and PNs have already been identified [13, 18, 19]. This minimal glomerular olfactory system exhibits the general

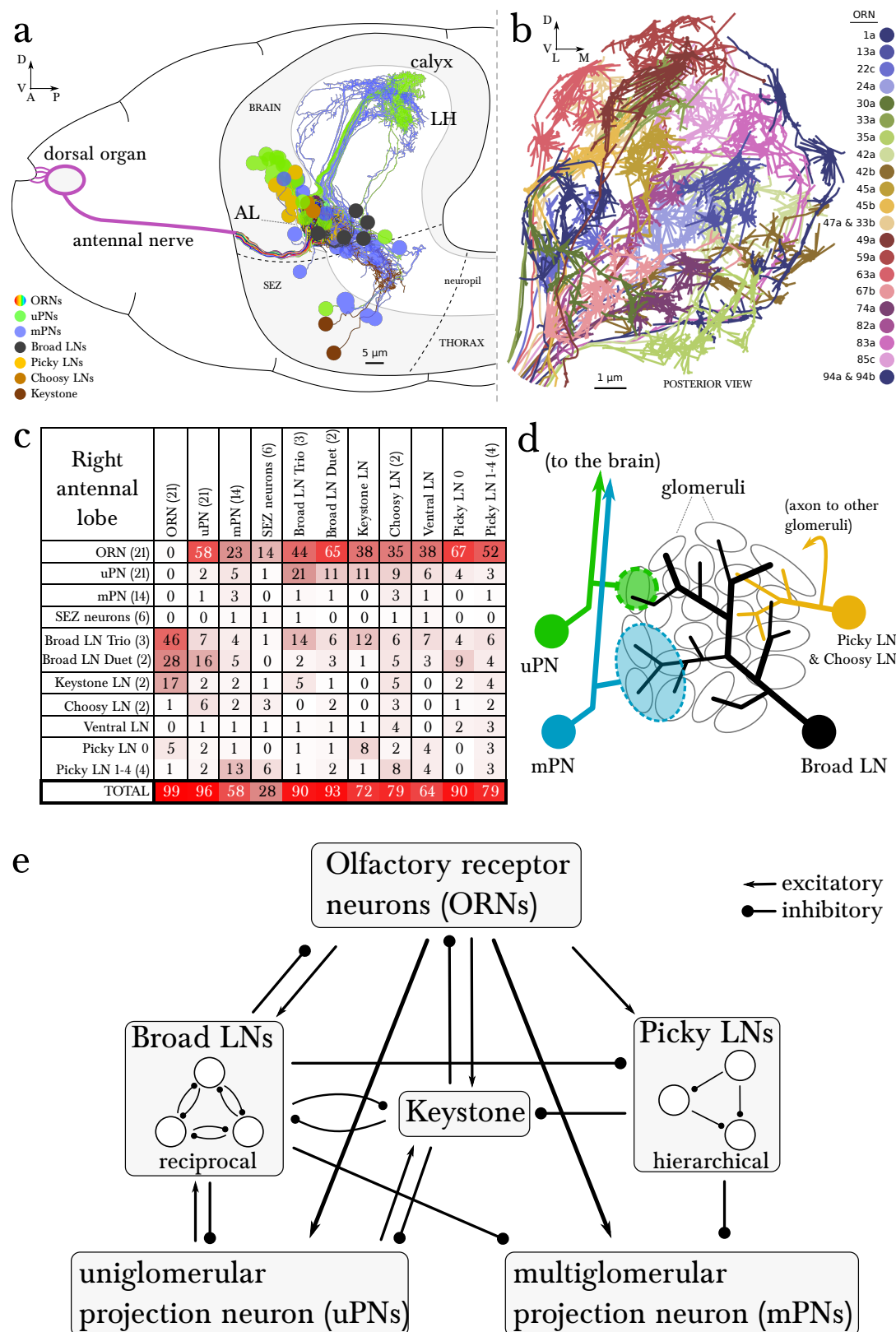


**Figure 1: (Continued.) D** Schematic of the innervation patterns of the main classes of LNs and PNs in the antennal lobe. White ovals represent the glomeruli. Solid circles are cell bodies. Shaded areas with dotted outlines represent the extent of the PN dendritic arbors, with each uPN (green) innervating one glomerulus and each mPN (blue) innervating multiple glomeruli. Their axons (arrows) project to the brain. Broad LNs (black) are axonless and present panglomerular arbors. Picky LN (orange) dendrites span multiple glomeruli and their axons (arrow; not shown) target a different yet overlapping set of glomeruli as well as regions outside the olfactory system. Choosy LNs are similar to the Picky LNs but their axons remain within the antennal lobe. **E** A simplified wiring diagram of the larval olfactory system with only the main connections. ORNs are excitatory. All shown LNs are inhibitory. Broad LNs reciprocally connect to all glomeruli and each other and thus engage in presynaptic inhibition (on ORNs) and postsynaptic inhibition (on uPNs). Picky LNs form a hierarchical circuit and selectively synapse onto mPNs. Another LN, Keystone, receives inputs from ORNs, one Picky LN and non-ORN sensory neurons, and can potentially alter the operational mode of the entire olfactory system by altering the pattern of inhibition (see text).

capabilities of the more numerically complex systems. For example, as in other organisms [20, 21] and in the adult fly [22–24], the output of the uniglomerular PNs tracks the ORN response [25], which represents both the first derivative of the odorant concentration and the time course of the odorant concentration itself [26]. Like in the adult fly [10] and zebrafish [27], gain control permits the larval olfactory system to operate over a wide range of odorant concentrations [25]. The olfactory behaviors exhibited by the larva have been well studied (mostly in 2nd and 3rd instar larvae), in particular chemotaxis [26, 28–33], as well as the odor tuning and physiological responses of ORNs [12, 25, 34–37]. Additionally the larva presents odor associative learning [38]. Obtaining the wiring diagram of all neurons synaptically connected to the ORNs would enable the formulation of system-level hypotheses of olfactory circuit function to explain the observed behavioral and functional properties. The reduced numerical complexity and dimensions of the larval olfactory system, the similarity of its organization and capabilities to other organisms, and the tractability of the larva as a transparent genetic model organism, make it an ideal model system in which to study the complete circuit architecture of a glomerularly organized olfactory processing center.

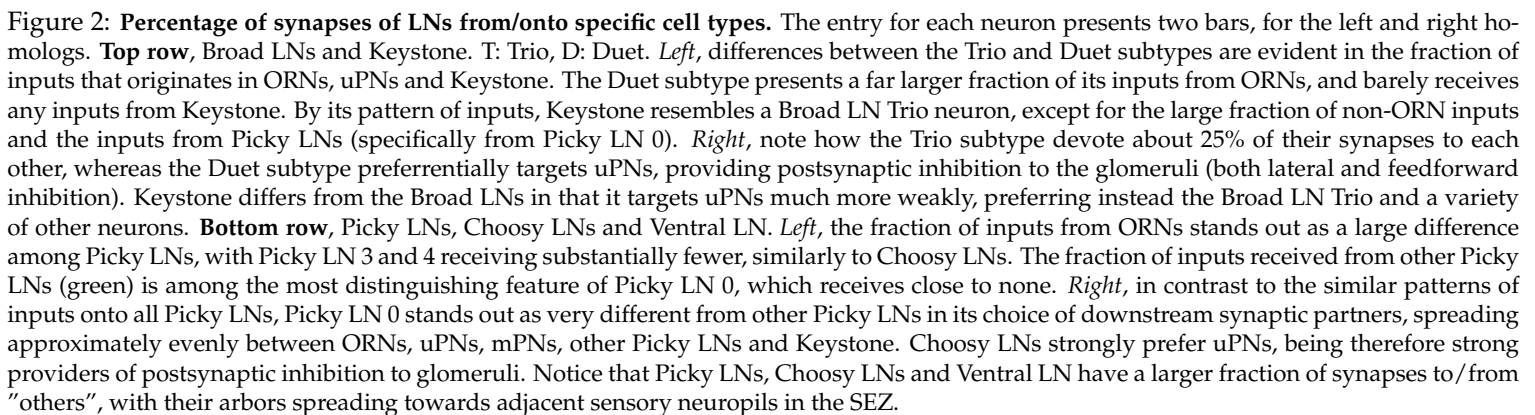
We reconstructed from electron microscopy all synaptic partners of the 21 ORNs for both the left and right antennal lobes of a first instar larva (Figure 1b; Figure 1-figure supplement 1 and 2). Per side, we found 21 uniglomerular PNs (uPNs; one per glomerulus), 14 LNs, 14 multiglomerular PNs (mPNs), 4 neuromodulatory neurons, 6 subesophageal zone (SEZ) interneurons and 1 descending neuron (Figure 1c, d). These identified neurons present stereotyped connectivity when comparing the left and right antennal lobes. The lack of undifferentiated neurons in the 1st instar antennal lobe, and comparisons with light-microscopy images of other instars suggests that the 1st instar antennal lobe contains all the neurons present throughout larval life. Here, we analyze this complete wiring diagram on the basis of the known function of circuit motifs in the adult fly and other organisms and known physio-

logical properties and behavioral roles of identified larval neurons. We found two distinct circuit architectures structured around the two types of PNs: a uniglomerular system where each glomerulus participates in a repeated, canonical circuit, centered on its uPN [39]; and a multiglomerular system where all glomeruli are embedded in structured, heterogeneous circuits read out by mPNs (Figure 1e; [19]). We also found that the inhibitory LNs structure a circuit that putatively implements a bistable inhibitory system. One state could compute odor saliency through panglomerular lateral inhibition, that is, by suppressing the less active glomeruli in favor of the more active ones. The other may enable select glomeruli, specialized for aversive odors, to respond to faint stimuli in a background of high, appetitive odor stimuli. We discuss the role of these two possible operational states and how neuromodulatory neurons and brain feedback neurons participate in the interglomerular circuits.

## Results

### Neurons of the olfactory system of *Drosophila* larva

We mapped the wiring diagram of the first olfactory neuropil of the larva by reconstructing the left and right ORNs and all their synaptic partners. We used a complete volume of the central nervous system (CNS) of a first instar larva, imaged with serial section electron microscopy ([17]; see methods for online image data availability; Figure 1-figure supplement 1). We reconstructed 160 neuronal arbors using the software CATMAID [40, 41]. All together, the 160 neurons add up to a total of 38,684 postsynaptic sites and 55 millimeters of cable, requiring about 600,000 mouse clicks over 736 hours of reconstruction and 431 hours of proofreading. Only 136 of 14,346 (0.9%) postsynaptic sites of ORNs remained as small arbor fragments (comprising a total of 0.25 millimeters of cable, or 0.5% of the total reconstructed) that could not be assigned to any neuron.





We sorted the 160 reconstructed neurons into 78 pairs of bilaterally homologous neurons and 4 ventral unpaired medial (VUM) neurons (2 are mPNs and 2 are octopaminergic “tdc” neurons; [42]). These 78 pairs we further subdivided into 21 pairs of ORNs, 21 pairs of uPNs, 13 pairs of mPNs (plus 2 additional VUM mPNs), 14 pairs of LNs, 6 pairs of neurons projecting to the SEZ (“SEZ neurons”), 1 pair of descending neurons from the brain, 1 pair of serotonergic neurons (CSD; [43]), and 1 pair of octopaminergic non-VUM neurons (“1AL-1”; [42]).

The 14 pairs of LNs originate in 5 different lineages (Figure 1-figure supplement 3). We assigned the same name to neurons of the same lineage, and numbered each when there is more than one per lineage. LNs connect to other neuron classes stereotypically in the two antennal lobes (Figure 2). We selected names reminiscent of either their circuit role or anatomical feature, including “Broad” to refer to panglomerular arbors; “Picky” and “Choosy” for LNs of two different lineages (and different neurotransmitter; see below) with arbors innervating select subsets of glomeruli; “Keystone” for a single pair that mediate interactions between LNs of different circuits; and “Ventral LN” for a single pair of LNs with ventral cell bodies. We also determined the neurotransmitters of LNs that were previously unknown (Figure 2-figure supplement 1). We introduce the properties of each LN type below with the olfactory circuits that they participate in.

## The uniglomerular system

In vertebrates and most arthropods, olfactory glomeruli are defined by a group of same-receptor ORNs converging onto a set of glomerular-specific PNs (mitral and tufted cells in the mouse and zebrafish olfactory bulb) [1, 3, 44–46]. In *Drosophila* larva, this system is reduced to a single ORN and a single uPN per glomerulus [13, 39, 47]. With one exception (35a, which has 2 bilateral uPNs), our EM-reconstructed wiring diagram is in complete agreement with these findings (Figure 1b, 3a). Most of the larval uPNs project to both the MB and the LH (Figure 3a), like in the adult fly [3, 48].

## Circuits for interglomerular inhibition

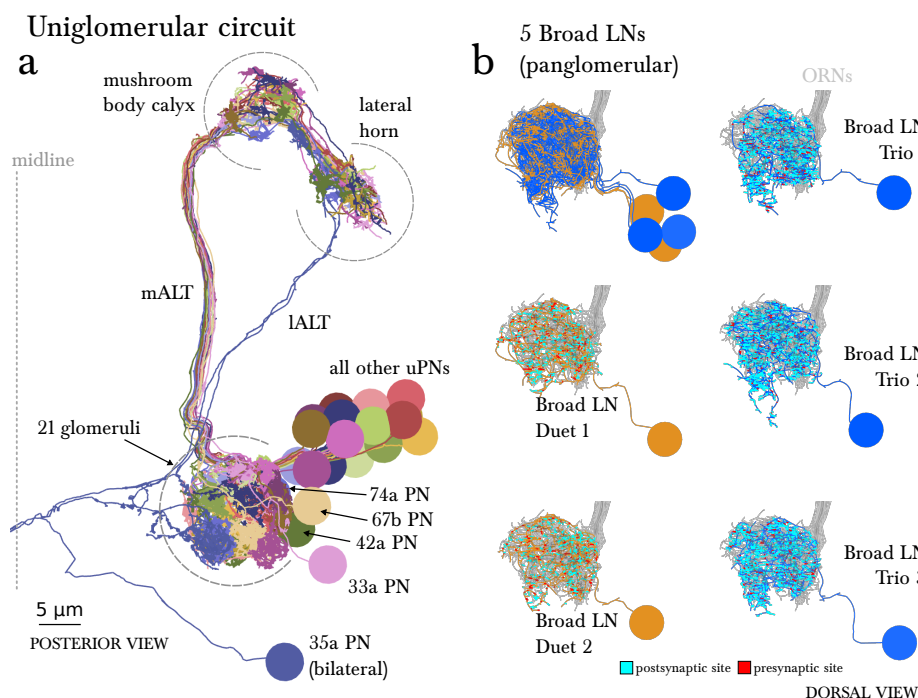
In insects (adult fly, bee, locust) and in vertebrates, the excitation of glomeruli is under control of inhibitory LNs that mediate functions such as gain control, which define an expanded dynamic range of uPN responses to odors [10, 27, 51–53]. We found that most non-sensory inputs to the larval uPNs (Figure

1c) are from a set of 5 panglomerular, axonless, and GABAergic [18] neurons that we named Broad LNs (Figure 3b, c; Figure 3-figure supplement 1). These 5 Broad LNs also account for most inputs onto the ORN axons (fig. 1c), therefore being prime candidates for mediating both intra- and interglomerular presynaptic inhibition (onto ORNs) as observed in the adult fly with morphologically equivalent cells [10, 53–55], and in the larva [25].

We divided the 5 Broad LNs into two classes, Trio and Duet, based on the number of neurons of each type (Figure 3b). While both types provide panglomerular presynaptic inhibition (onto ORN axons), the Duet makes far more synapses onto the dendrites of the uPNs. This may indicate a far stronger role for the Broad LN Duet in postsynaptic inhibition (onto uPN dendrites; Figure 3d). In the adult fly, presynaptic inhibition implements gain control [10], and postsynaptic inhibition plays a role in uPNs responding to the change in ORN activity [24, 56]. The two types of glomerular inhibition are provided by two separate cell types, and may therefore be modulated independently. For example, the uPNs emit dendritic outputs that primarily target the Broad LN Trio (Figure 3d), indicating that the output of the glomerulus contributes more to presynaptic than to postsynaptic inhibition. Similar excitatory synapses from uPNs to inhibitory LNs have been shown in vertebrates [57], and synapses from PNs to LNs and vice versa have been described in the adult fly [11].

Beyond their role in pre- and postsynaptic inhibition of ORNs and uPNs respectively, the Broad LNs synapse onto all neurons of the system, including other LNs and mPNs (Figure 1c, Figure 2). Therefore Broad LNs may be defining a specific dynamic range for the entire antennal lobe, enabling the system to remain responsive to changes in odorant intensities within a wide range. Importantly, Broad LNs also synapse onto each other (Figure 3c, e) like in the adult [11, 58]. Furthermore, the two types of Broad LNs have a different ratio of excitation and inhibition, originating in the preference of Trio to synapse far more often onto each other than onto Duet (Figure 3e, Figure 2). This suggests that the two types not only have different circuit roles but also have different properties.

Another GABAergic cell type, that we call the Choosy LNs (two neurons; Figure 1c, 3c, Figure 1-figure supplement 3), contributes exclusively to postsynaptic inhibition for most glomeruli. Unlike the Broad LNs, Choosy LNs have a clear axon innervating most glomeruli, while their dendrites collect inputs from only a small subset of glomeruli (Figure 3c; Figure 1-figure supplement 3; Figure 3-figure supplement 1). Therefore some



**C** Percent of postsynaptic inputs of a column neuron from a row neuron

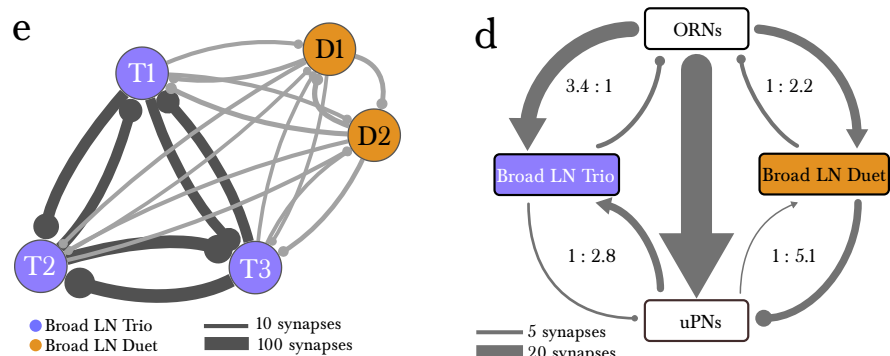
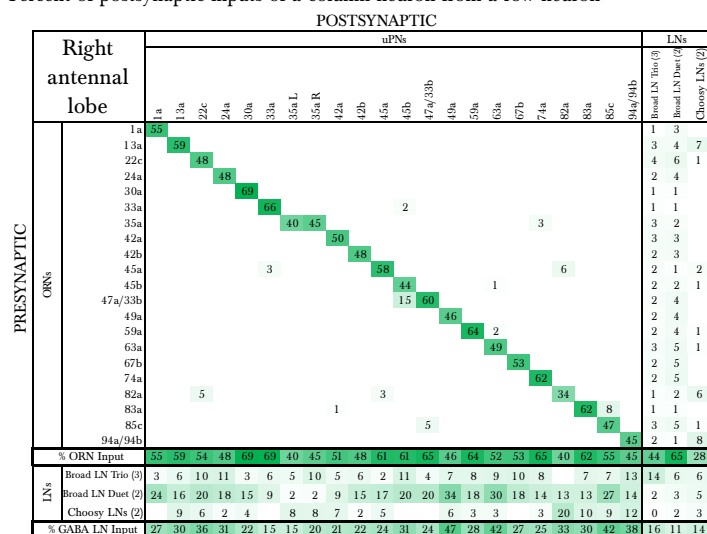


**Figure 3: The uniglomerular circuit consists of 21 glomerular-specific projection neurons, which interact primarily with their corresponding ORN and with the 5 panglomerular LNs (Broad LNs), each an identified neuron.** A Posterior view of the EM-reconstructed uPNs of the right antennal lobe. The dendrites of each uPN delineate the glomerular boundaries, and the axons project to both the mushroom body (required for learning and memory; [49]) and the lateral horn (implicated in innate behaviors; [50]). 19 uPNs are likely generated by the same neuroblast lineage BAMv3 [19] (although the uPNs for 42a, 74a, and 67b are slightly separated from the rest), and the other two (the uPNs for 33a and 35a) clearly derive from two other neuroblasts. Notice that the 35a uPN is bilateral, ascends through a different tract, and receives additional inputs outside of the antennal lobe. The 33a uPN does not synapse within the calyx and the 82a uPN does not continue to the lateral horn. The left antennal lobe (not shown) is a mirror image of the right one. **B** Dorsal view of the EM-reconstructed, axonless Broad LNs (Duet in orange; Trio in blue) shown together and individually. All neurons are on the same lineage: BALc [19]. The pre-(red) and post-(cyan) synaptic sites on these panglomerular neurons are fairly uniformly distributed. ORNs in grey for reference. These neurons extend posteriorly out of the olfactory glomeruli to receive synapses from 2 non-ORN sensory neurons that enter the brain via the antennal nerve. **C** Percentage of the total number of postsynaptic sites on the dendrite of an uPN, Broad LN or Choosy LN (columns) that originate in a given ORN or LN (rows) for the right antennal lobe. Since the 35a uPN is bilateral, we include inputs to it from both antennal lobes. We show only connections with at least two synapses, consistently found among homologous identified neurons in both the left and right antennal lobes. Percentages between 0 and 1 are rounded to 1, but totals are computed from raw numbers. The uniglomerular nature of uPNs (notice the green diagonal) and panglomerular nature of Broad LNs is evident. The Broad LN Duet generally contributes more synapses onto uPNs than the Broad LN Trio does. While the number of synapses that an ORN makes onto its uPN varies widely (24-120 synapses; see Supplementary File 1 and 2), this number is tailored to the size of the target uPN dendrite given that percentage of inputs the ORN contributes to the uPN is much less varied (mostly 45-65%). For an extended version of this table that includes all LNs, see Figure 3-figure supplement 1. **D** Both Broad LN types (Trio and Duet) mediate presynaptic inhibition (synapses onto ORN axons) similarly, but the Duet shows far stronger postsynaptic inhibition (synapses onto uPN dendrites) while the Trio receives far more dendro-dendritic synapses from uPNs. Connections among Broad LNs are not shown for simplicity. Each arrow is weighted linearly by the number of synapses for an average single Broad LN of each type. **E** The 5 Broad LNs that govern this circuit synapse reciprocally, with the Trio type synapsing more strongly onto each other. Shown here for the right antennal lobe with arrow thickness weighted by the square root of the number of synapses.

glomeruli can drive postsynaptic inhibition of most glomeruli. Additionally, the inputs from Choosy LNs tend to be more proximal to the axon initial segment of the uPNs [59] unlike those of Broad LNs which are more uniformly distributed throughout the uPN dendritic arbor (Figure 3-figure supplement 2). In the adult, ORNs tend to synapse at the most distal PN dendritic terminals, allowing for some LN inhibition to occur via synapses more proximal to the axon initial segment [11]. This pattern of spatially structured inputs suggests that different inhibitory LN types may exert different effects on uPN dendritic integration.

## The multiglomerular system

Parallel to the uniglomerular readout by the 21 uPNs, we found 14 multiglomerular PNs (mPNs; Figure 4a). Each mPN receives unique and stereotyped inputs from multiple ORNs (Figure 4c) or at least from one ORN and multiple unidentified non-ORN sensory neurons in the SEZ (Figure 4a). The mPNs originate in multiple neuronal lineages and project to multiple brain regions; most commonly the lateral horn (LH) but also regions surrounding the MB calyx. Of the 14 mPNs, three project to the calyx itself (mPNs b-upper, b-lower and C2) and another (mPN cobra) to the MB vertical lobe (Figure 4a). In addition to the 14 mPNs that project to the brain, we identified an extra 6 oligoglomerular neurons that project to the SEZ (SEZ neurons; Figure 1c; Figure 4-figure supplement 1). A class of mPNs has been described in the adult fly [4] but their projection pattern does not match any of the larval mPNs. In strong contrast to uPNs, mPNs are very diverse in their lineage of origin, their pattern of inputs, and the brain areas they target. A small subset of mPNs has been identified via light microscopy before [18, 19].

In addition to inputs from Broad LNs (Figure 4-figure supplement 2), mPNs also receive up to 26% of inputs from 5 stereotypically connected, oligoglomerular LNs that we call Picky LNs (Figure 4b, c). While both Choosy LNs and Picky LNs are oligoglomerular and present distinct axons, the Choosy LNs are GABAergic whereas at least 4 of the 5 Picky LNs are instead glutamatergic (Figure 2-figure supplement 1 for Picky LNs and Fig. 2 panels L-O in [18] for Choosy LNs; see also Supp. Fig. 2 of [19]). The difference in neurotransmitter is consistent with Picky LNs deriving from a different lineage than Choosy LNs (Figure 1-figure supplement 3). In addition, the two Choosy LNs present indistinguishable connectivity, whereas each Picky LN has its own preferred synaptic partners (see Supplementary File 1 and 2). Additionally, unlike the Choosy LNs, Picky LNs rarely target uPNs (Figure 3-figure supplement 1). Glutamate

has been shown to act as a postsynaptic inhibitory neurotransmitter in the adult fly antennal lobe for both PNs and LNs [60], and therefore in larva, Picky LNs may provide inhibition onto both mPNs and other LNs. Unlike the Broad LNs, which are panglomerular and axonless, the Picky LNs present separated dendrites and axons (Figure 4b). Collectively, Picky LN dendrites roughly tile the antennal lobe (Figure 4b). While some Picky LN axons target select uPNs, about 40% of Picky LN outputs are dedicated to mPNs or each other (Figure 4c; Figure 2). Similarly to the mPNs, Picky LNs 2, 3, and 4 receive inputs from unidentified non-ORN sensory neurons in the SEZ (Figure 4b, Figure 2).

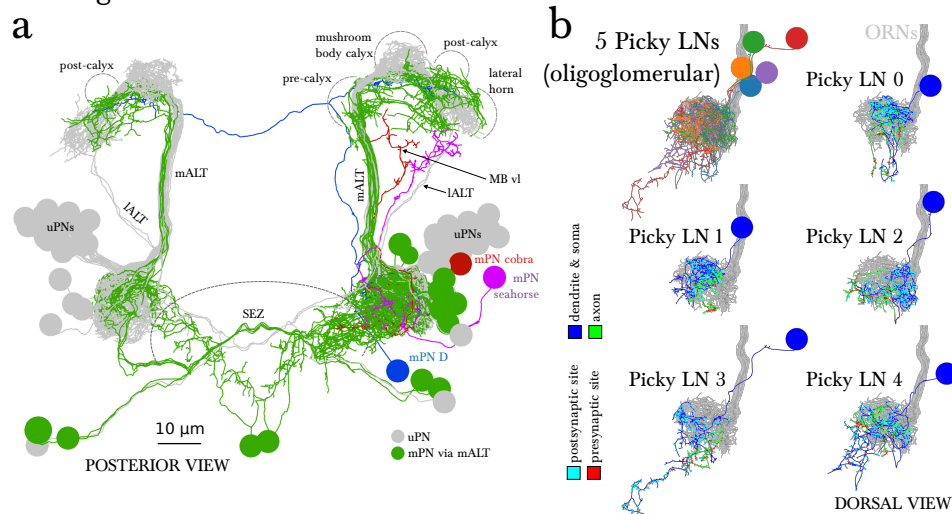
Given that ORNs present overlapping odor tuning profiles [35], we applied dimensionality-reduction techniques and discovered that ORNs cluster into 5 groups by odorant preference (Figure 4-figure supplement 3; see the Materials and Methods section for more detail). This helped interpret the pattern of ORNs onto Picky LNs and mPNs. We found that some Picky LNs aggregate similarly responding ORNs (Figure 4d; Figure 4-figure supplement 4). For example, Picky LN 2 receives inputs preferentially from ORNs that respond to aromatic compounds, and Picky LN 3 and 4 similarly for aliphatic compounds (esters and alcohols; Figure 4-figure supplement 4). On the other hand, Picky LN 0 and 1 aggregate inputs from ORNs from different clusters, suggesting that these Picky LNs may select for ORNs that are similar in a dimension other than odorant binding profile.

The stereotyped and unique convergence of different sets of ORNs onto both mPNs and Picky LNs, and the selective connections from Picky LNs to mPNs, suggest that each mPN responds to specific features in odor space, defined by the combinations of ORN and Picky LN inputs. These features are implemented through direct excitatory connections from ORNs or indirect inhibitory connections via Picky LNs (lateral inhibition; Figure 4d). Some ORNs affect the activity of the same mPN through both direct excitatory and lateral inhibitory connections through Picky LNs (incoherent feedforward loop, [61]; Figure 4d). The combination of these motifs may enable an mPN to respond more narrowly to odor stimuli than the ORNs themselves, many of which are broadly tuned [35], or to respond to a combinatorial function of multiple ORNs that describe an evolutionarily learned feature meaningful for the larva.

For example, one mPN (A1) reads out the total output of the uniglomerular system by integrating inputs across most ORNs and uPNs (Figure 4c). Another mPN (B2) could respond to the linear combination of ORNs sensitive to aromatic com-



## Multiglomerular circuit



## C Percent of postsynaptic inputs of a column neuron from a row neuron

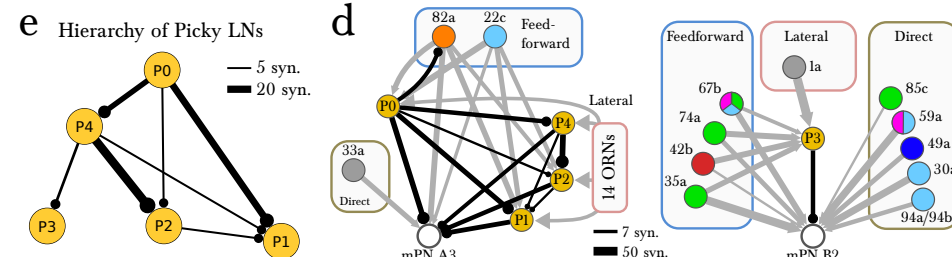
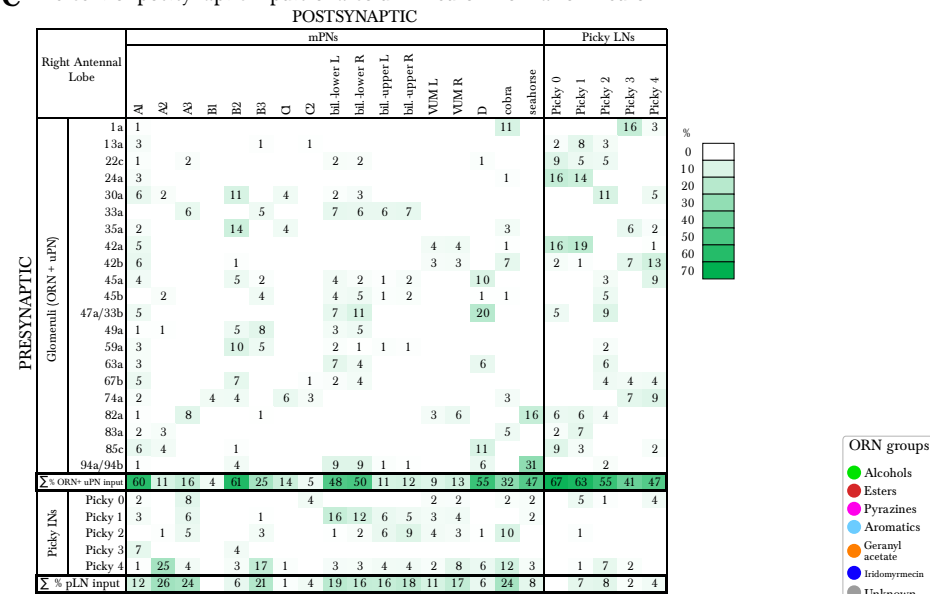


**Figure 4: The multiglomerular circuit consists of 14 mPNs that project to the brain and 5 Picky LNs, each an identified neuron.** A Posterior view of EM-reconstructed mPNs that innervate the right antennal lobe (in color; uPNs in grey for reference), each receiving inputs from a subset of olfactory glomeruli but many also from non-ORN sensory neurons in the subesophageal zone (SEZ). Most mPNs (green) project via the same tract as the uPNs (mALT). They can project via other tracts (other colors), but never via the mALT used by the iPNs of the adult *Drosophila*. The mPNs project to many regions including a pre-calyx area, a post-calyx area, the lateral horn (LH) and the mushroom body vertical lobe (MB vl). mPNs are generated by diverse neuroblast lineages including BALp4, BALa1, and others [19]. **B** Dorsal view of the EM-reconstructed Picky LNs shown together and individually. When shown individually, the Picky LNs are in 2 colors: blue for the dendrites and soma, and green for the axon. Zoom in to observe that presynaptic sites (red) are predominantly on the axon, whereas postsynaptic sites (cyan) are mostly on dendrites. Collectively, the dendritic arbors of the 5 Picky LNs tile the olfactory glomeruli. The dendrites of the Picky LN 3 and 4 extend significantly into the SEZ. They all originate from the same neuroblast lineage: BALa2 [19]. **C** Percentage of the total number of postsynaptic sites on the dendrite of a mPN or Picky LN (column neuron) that originate from a given glomerulus or Picky LN (row neurons). Here we define the glomerulus as connections from the ORN or via dendro-dendritic synapses from a given ORN's uPN. This is most relevant for mPN A1, which can receive more synapses from an ORN's uPN than the ORN itself (see suppl. Adjacency Matrix). We show the inputs to the mPNs and Picky LNs for the right antennal lobe, but for all bilateral mPNs (bil.-lower, bil.-upper, and VUM) we include inputs from both sides. We show only connections with at least two synapses, consistently found among homologous identified neurons in both the left and right antennal lobes. Percentages between 0 and 1 are rounded to 1, but totals are computed from raw numbers. Connections in this table are stereotyped (when comparing the left and right antennal lobes) and selective. Note that mPNs that receive many inputs from non-ORN sensory neurons in the SEZ have a low total of ORN+uPN input. For an extended version of this table that includes all LNs see Figure 4-figure supplement 2.

**D** The direct upstream connectivity for two mPNs, with ORNs colored by the groups emerging from the PCA analysis of odor tuning. Connections from ORNs and Picky LNs to mPNs create 3 different types of motifs: *direct* excitatory connections from ORNs, *lateral* inhibitory connections from ORNs only via Picky LNs, and *feedforward* loops where an ORN connects both directly to the mPN and laterally through a Picky LN. Note that the activity of Picky LN 0 could alter the integration function for mPN A3 and indirectly for B2, as well as many other mPNs (not shown). Arrow thicknesses are weighted by the square root of the number of synapses between neurons. **E** The Picky LN hierarchy, dominated by Picky LN 0, here showing connections with 2 or more consistent synapses between bilaterally homologous neurons. Some of these connections are axo-axonic (see Figure 4-figure supplement 4).



pounds (direct connections), but its response could change in the presence of alcohols and esters due to feedforward loops (Figure 4d). And mPNs A3 and B3 both collect inputs from ORNs (Figure 4c, d) known to respond to aversive compounds (22c, 45b, 49a, 59a, and 82a; [35, 62]) or whose ORN drives negative chemotaxis (45a; [29, 33]). Additionally, mPN B3 receives inputs from 33a, an ORN whose receptor lacks a known binding compound, and therefore is likely narrowly tuned to other ecologically relevant odorants as was shown for 49a and the pheromone of a parasitic wasp [62]. The connectivity patterns of the 14 types of mPNs are vastly diverse from each other and likely each one extracts different features from odor space, often integrating inputs from non-ORN sensory neurons as well.

In contrast to the all-to-all connectivity of the Broad LNs, the Picky LNs synapse onto each other in a selective, hierarchical fashion (Figure 4e). The structure of the Picky LN hierarchy suggests that Picky LNs 0 and 3 can operate in parallel, while the activity of the other Picky LNs is dependent on Picky LN 0 (Figure 4e). These connections among Picky LNs include axo-axonic connections, and some Picky LNs receive stereotypic ORN inputs onto their axons (Figure 4-figure supplement 4). The stereotyped hierarchy among Picky LNs defines yet another layer of computations in the integration function of each mPN.

## Non-ORN sensory neurons and interactions among LNs could alter the operational state of the olfactory system

Picky LN 0 not only dominates the Picky LN hierarchy, and with it the multiglomerular system, but also may dramatically alter the inhibition of the entire olfactory system. This is because the main synaptic target of Picky LN 0 (Figure 2) is a bilateral, axonless, GABAergic LN called Keystone (Figure 5a; Figure 2-figure supplement 1), which in turn strongly synapses onto the Broad LN Trio—a major provider of presynaptic inhibition (Figure 5b). Interestingly, Keystone is also a major provider of presynaptic inhibition, but selectively avoids some glomeruli (Figure 5c; Figure 3-figure supplement 1). Therefore the wiring diagram predicts that these two parallel systems for presynaptic inhibition can directly and strongly inhibit each other (Figure 5b): homogeneous across all glomeruli when provided by the Broad LN Trio, and heterogeneous when provided by Keystone (Figure 5c). In conclusion, the circuit structure and the known synaptic signs predict that Picky LN 0 can promote a state of homogeneous presynaptic inhibition by disinhibiting the Broad LN Trio (Figure 5d).

The alternative state of heterogeneous presynaptic inhibition implemented by Keystone could be triggered by select non-ORN sensory neurons that synapse onto Keystone in the SEZ (Figure 5a, b). These non-ORN sensory neurons are the top inputs of Keystone and do not synapse onto any other olfactory LN. In contrast, ORNs that synapse onto Keystone also synapse onto the Broad LN Trio (Figure 3-figure supplement 1), suggesting a role for non-ORN sensory inputs in tilting the balance towards Keystone and therefore the heterogeneous state. However, the subset of ORNs that also synapse onto Picky LN 0 (Figure 4c) could oppose the effect of the non-ORN sensory neurons by inhibiting Keystone and therefore disinhibiting the Broad LN Trio.

Neuromodulatory neurons could also affect the balance between Keystone and Broad LN Trio. Beyond the possible effect of volume release of serotonin [64] and octopamine [63, 65] within the olfactory system, we found that these neuromodulatory neurons synapse directly and specifically onto Keystone or Broad LN Trio, respectively (Figure 5b). Beyond non-ORN inputs, ORNs synapse selectively onto these neuromodulatory neurons. Two ORNs (74a and 82a) synapse onto the serotonergic neuron CSD [43], and five ORNs (42b, 74a, 42a, 35a and 1a) onto an octopaminergic neuron (IAL-1; see fig. 4k in [42]), suggesting that specific ORNs may contribute to tilting the balance between homogeneous and heterogeneous presynaptic inhibition, as well as exert further effects via neuromodulation.

The only other provider of panglomerular presynaptic inhibition is the Broad LN Duet, which is the main provider of panglomerular postsynaptic inhibition. These neurons may operate similarly in both states given that they are inhibited by both Keystone and Broad LN Trio (Figure 1c). The higher fraction of inputs from Broad LN Trio onto Duet might be compensated by the fact that the Trio LNs inhibit each other (Figure 3e, 5b), whereas the two Keystone LNs do not (Figure 5b). Therefore, potentially the Broad LN Duet could be similarly active in either state (Figure 5d).

## Some glomeruli are special-purpose

The possibility of heterogeneous presynaptic inhibition promoted by Keystone suggests that some ORNs can escape divisive normalization of their outputs relative to the rest. Not surprisingly, one such ORN is 49a (Figure 5c), which is extremely specific for the sexual pheromone of a parasitic wasp that predates upon larvae [62]. The other two ORNs that escape fully are 1a and 45b. 1a activation drives negative chemotaxis

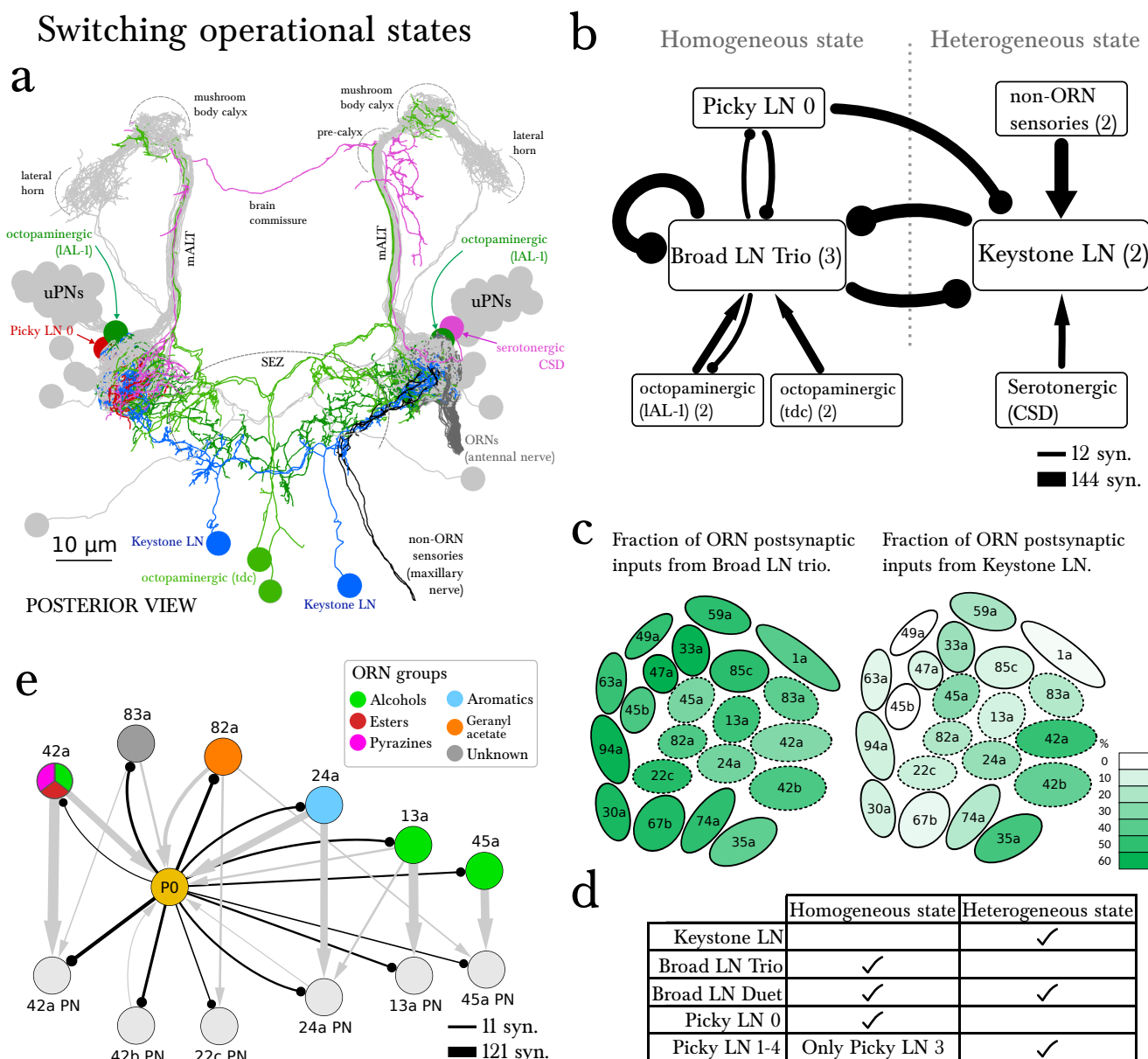


**Figure 5: The wiring diagram suggests two operational states: homogeneous or heterogeneous presynaptic inhibition.** **A** Posterior view of the EM-reconstructed neurons innervating the left antennal lobe that could govern the switch (uPNs in grey and right ORNs in dark grey for reference). The Keystone LN (blue) has a symmetric bilateral arbor and additionally innervates the SEZ, receiving inputs from non-ORN sensory neurons (in black). Neuromodulatory neurons that make direct morphological synapses onto LNs are serotonergic (CSD in pink; projects contralaterally after collecting inputs from near the MB calyx) and octopaminergic (IAL-1 and two tdc, in dark and light green), and all arborize well beyond the antennal lobe. Also included is Picky LN 0 (red). **B** A wiring diagram outlining the strong LN-LN connections, showing the core reciprocal inhibition between Broad LN Trio and Keystone that could mediate the switch between homogeneous (panglomerular) presynaptic inhibition and heterogeneous (selective) presynaptic inhibition. For simplicity, neurons are grouped together if they belong to the same neuron type, with the number of neurons belonging to each group indicated in parentheses. Connections are weighted by the square root of the number of synapses between groups of neurons. The self-arrow for the Broad LN Trio represents the average number of synapses that one of the Trio neurons receives from the other two. Picky LN 0 inhibits Keystone, thereby disinhibiting the Broad LN Trio and promoting homogeneous presynaptic inhibition. The maxillary nerve sensory neurons are the top input providers of Keystone and may drive the system towards heterogeneous presynaptic inhibition (see **C**). The effect of direct inputs from neuromodulatory neurons is unknown, but at least it has been suggested that octopaminergic neurons may have an excitatory effect on inhibitory LNs [63]. **C** Cartoon of glomeruli colored by the percentage of inputs onto ORN axon terminals provided by the Broad LN Trio and from Keystone, indicating the amount of presynaptic inhibition (onto ORNs) in either state. The inhibition provided by Broad LN Trio is much more uniform than the inhibition provided by Keystone. Dotted lines indicate glomeruli that receive Picky LN 0 input on either the ORN or uPN. **D** The LNs putatively active in each state. **E** Unlike other Picky LNs, Picky LN 0 makes synapses onto ORN axon terminals and many uPNs. Here connections with 2 or more synapses consistent between bilaterally homologous neuron pairs are shown. Arrow thicknesses are weighted by the square root of the number of synapses between neurons. With the exception of 45a, all shown ORNs and uPNs belong to glomeruli that synapse onto Picky LN 0 as well. Thus Picky LN 0 provides both pre- and postsynaptic inhibition to a small set of glomeruli.

(Hernandez-Nuñez et al., unpublished). 45b senses compounds that elicit negative chemotaxis in larvae [35]. These three ORNs, and in particular 49a, are under strong postsynaptic inhibition by both Broad LN Duet and Choosy LNs (Figure 3c). In summary, reducing presynaptic inhibition in these 3 ORNs may enable larvae to perceive odors evolutionarily associated with life-threatening situations less dependently of the response intensity of other ORNs (i.e. overall odorant concentration). This is consistent with the finding that responses to aversive odors may rely on specific activity patterns in individual ORNs [66]. The strong postsynaptic inhibition might be instrumental for their corresponding uPN to respond to the derivative of the ORN activity (with an incoherent feedforward loop; [61]), as shown in the adult fly [24], facilitating detection of concentration changes.

A key neuron in tilting the balance between homogeneous and heterogeneous presynaptic inhibition in the Broad-Keystone circuit is Picky LN 0 (Figure 5b). Remarkably, one of the two top ORN partners of Picky LN 0 is ORN 42a (Figure 4c), the strongest driver of appetitive chemotaxis in larvae [12, 25, 26, 33]. The connections of Picky LN 0 extend beyond that of other oligoglomerular LNs, and include both pre- and postsynaptic inhibition of a small subset of glomeruli, including 42a (Figure 5e). The wiring diagram therefore indicates that Picky LN 0, a likely glutamatergic LN, engages in seemingly contradictory circuit motifs: simultaneously inhibiting specific ORNs and their uPNs, while also disinhibiting them by inhibiting Keystone. The suppression of Keystone disinhibits the Broad LN Trio and therefore promotes homogeneous inhibition. However this is further nuanced by reciprocal connections between Picky LN 0 and Broad LN Trio (Figure 5b). This push-pull effect of glutamatergic LNs on PN has been described for the olfactory system of the adult fly as conducive to more robust gain control and rapid transitions between network states [60]. This refined control could endow Picky LN 0-innervated glomeruli like 42a (Figure 5e) with the ability to better detect odor gradients, consistent with 42a being a strong and reliable driver of appetitive chemotaxis [12, 25, 26].

Picky LN 0 and its push-pull effect on PN not only can have an effect on positive chemotaxis but also on negative. A clear example is the 82a glomerulus (known to respond to an aversive odor that drives negative chemotaxis [35]) which lacks a well-developed uPN but engages in strong connections with mPNs such as A3 (Figure 4c,d). We found that, like for the appetitive case of 42a, Picky LN 0 engages in both presynaptic inhibition onto 82a ORN and also postsynaptic inhibition onto mPN A3, one of the top PN of 82a ORN. And like other ORNs

mediating aversive responses (e.g 49a), the 82a uPN is also under strong postsynaptic inhibition (Figure 3c).

Finally, we found evidence that an individual glomerulus can have a global effect on the olfactory system. All LNs (except Picky LN 3) receive inputs from Ventral LN (Figure 1c, Figure 3-figure supplement 1), an interneuron of unknown neurotransmitter, which is primarily driven by the 13a glomerulus. This suggests that 13a, an ORN sensitive to alcohols [35], could potentially alter the overall olfactory processing.

## Feedback from the brain

In the mammalian olfactory bulb, descending inputs from the brain target granule cells (the multiglomerular inhibitory LNs), shaping the level of inhibition [67]. In addition to descending neuromodulatory neurons (CSD; Figure 5a), in the larva we found a descending neuron (Figure 5-figure supplement 1) that targets specific mPNs and LNs (Figure 4-figure supplement 2). In addition to other mPNs, this descending neuron targets the two mPNs that we postulate are aversive (mPNs A3 and B3). Together with the axo-axonic inputs it receives from 45a ORN (an aversive ORN, [29, 33]), this descending neuron is associated with the processing of aversive stimuli. Additional descending neurons affecting PN and LNs might exist but were beyond the scope of this study, where we focused on neurons directly synapsing with ORNs.

## Discussion

The glomerular olfactory system of the larva develops in a similar fashion to the vertebrate olfactory bulb where the afferents (i.e. ORNs) organize the central neurons, unlike in the adult fly [68]. In zebrafish, GABAergic LNs provide depolarizing currents to PN (mitral cells) via gap junctions at low stimulus intensities, enhancing low signals, and inhibit the same PN at high stimulus intensity via GABA release, implementing a form of gain control [27]. This role is played by a class of panglomerular excitatory LNs in the adult fly that make gap junctions onto PN and excite inhibitory LNs [69]. In the larva, all panglomerular neurons are GABAergic; if any were to present gap junctions with uPNs, a cell type for gain control in larva would be equivalent to the one in zebrafish. Particularly good candidates are the Broad LN Duet, which provide the bulk of feedforward inhibitory synapses onto uPNs in larva. Interestingly, postsynaptic inhibition might not be mediated by GABA in the adult fly

(supp. fig. 5 in [10]), rendering olfactory circuits in larva more similar to vertebrates. Presynaptic inhibition exists both in the adult fly and, as suggested by the present work, in larva, and is mediated by the same kind of panglomerular GABAergic neurons (the Broad Trio LNs in larva; and see [10]).

The uniglomerular circuit is the most studied in all species both anatomically and physiologically. We found that each uPN receives an unusually large number of inputs from an individual ORN compared to other sensory systems in the larva [17]. This large number of morphological synapses could be interpreted as a strong connection, which would support faster or more reliable signal transmission. In the adult fly, the convergence of multiple ORNs onto an individual PN enables both a fast and reliable PN response to odors [22]). The temporal dynamics of crawling are far slower than that of flying, and therefore we speculate that the integration over time of the output of a single ORN might suffice for reliability, demanding only numerous synapses to avoid saturation.

Positive, appetitive chemotaxis involves odor gradient navigation, leading to a goal area where food is abundant which may overwhelm olfaction. We postulate that navigation and feeding correspond to the homogeneous and heterogeneous states of presynaptic inhibition that we described. During navigation, homogeneous presynaptic inhibition (via Broad LN Trio) could best enhance salient stimuli and therefore chemotaxis, enabling the olfactory system to operate over a wide range of odorant intensities [25]. During feeding, strongly stimulated ORNs could scale down the inputs provided by other, less stimulated, ORNs. In other words, if homogeneous presynaptic inhibition persisted during feeding, the larvae would lose the ability to detect important odorants that are likely to be faint, for example the scent of a predator such as a parasitic wasp via 49a [62]. The larva can selectively release presynaptic inhibition via Keystone, which provides presynaptic inhibition to appetitive glomeruli while also inhibiting the Broad LN Trio—the major providers of panglomerular presynaptic inhibition. So the larva could feed and remain vigilant to evolutionarily important cues at the same time. Not surprisingly, the switch might be triggered by neuromodulatory neurons and non-ORN sensory neurons, potentially gustatory, that synapse onto Keystone.

In addition to the uniglomerular system that is present across multiple vertebrate and invertebrate species [1, 2, 44], we found, in the *Drosophila* larva, a multiglomerular system that presumably performs diverse processing tasks already at the first synapse. One such task could be the detection of concentration gradients for some odorant mixtures, suggesting an ex-

planation for the observation that some ORNs can only drive chemotaxis when co-activated with other ORNs [12]. Similar glomerular-mixing circuits have been described in higher brain areas (lateral horn) of the fly [70, 71] and of mammals [9]. We hypothesize that in the larva, the morphological adaptations to a life of burrowing might have led to specific adaptations, relevant to an animal that eats with its head, and therefore the dorsal organ housing the ORNs, immersed in food. It is perhaps not surprising that we found multisensory integration across ORNs and non-ORNs (likely gustatory) already at the first synapse. And we hypothesize that the pooling of chemosensors (ORNs and non-ORNs) onto mPNs and Picky LNs may be related to the reduction in the number of ORNs relative to insects with airborne antennae.

With our complete wiring diagram of this tractable, transparent model system and genetic tools for manipulating and monitoring the activity of single identified neurons, we have now the opportunity to bridge the gap between neural circuits and behavior [72].

## Materials and methods

### Electron microscopy and circuit reconstruction

We reconstructed neurons and annotated synapses in a single, complete central nervous system from a 6-h-old [*iso*] *Can- ton S G1 x w<sup>1118</sup>* larva imaged at 4.4 x 4.4 x 50 nm resolution, as described in [17]. The volume is available at <http://openconnecto.me/catmaid/>, titled "acardona.0111.8". To map the wiring diagram we used the web-based software CATMAID [40], updated with the novel suite of neuron skeletonization and analysis tools [41], and applied the iterative reconstruction method described in [17, 41].

### Immunolabeling and light microscopy

CNS was dissected from 3rd instar larvae. 4% formaldehyde was used as fixative for all antibodies except anti-dVGlut that required bouin fixation [73]. After fixation, brain samples were stained with rat anti-flag (1:600, Novus Biologics) and chicken anti-HA (1:500, Abcam, ab9111) for labeling individual neurons in the multi-color flip-out system [74], while mouse anti-Chat (1:150, Developmental Studies Hybridoma Bank, ChaT4B1) and rabbit anti-GABA (1:500, Sigma A2052, Lot# 103M4793) or anti-dVGlut [75] were used for identifying neurotransmitters. Anti-



bodies were incubated at 4°C for 24 hours. Preparations were then washed 3 times for 30 min. each. with 1% PBT and then incubated with secondary antibodies (including: goat anti-Mouse Alexa Fluor 488, goat anti-rabbit Alexa Fluor 568, donkey anti-rat Alexa Fluor 647, Thermofisher; and goat anti-chicken Alexa Fluor 405, Abcam) at 1/500 dilution for 2 hours at room temperature, followed by further washes. Nervous systems were mounted in Vectashield (Vector Labs) and imaged with a laser-scanning confocal microscope (Zeiss LSM 710).

## Clustering of ORNs by PCA of their responses to odors

Extensive screens have been conducted to identify which odorants activate each ORN [35–37]. These data can be used as a starting point to determine whether the multiglomerular circuit extracts relevant components of odorant physical descriptor space, that is, the chemical structure of the odorant as sampled by ORNs. Using the data from [35] and [36], we conducted a dimensionality reduction via PCA followed by a clustering analysis, and then used the data from [37] to verify our findings. To determine how ORNs encode odors we followed the PCA analysis in ORN space performed in [76] adding the data of pyrazines from [36]. Then, using the Scree test we selected the first 3 components of the PCA as the relevant ones to use for clustering, and we ran the clustering minimization using the affinity propagation algorithm (which doesn't require the number of clusters as an input) (Figure 4-figure supplement 3b, c). Four of the obtained clusters correspond very well with odorant type (alcohols, aromatics, esters, and pyrazines; Figure 4-figure supplement 3d). The fifth cluster is mixed and mainly includes odorants with very low or no ORN response. Consistent with that, k-means clustering in the 32-dimensional odorant physical descriptor space described in [77] results in 5 clusters, 4 of them matching the non-mixed clusters obtained in ORN space (Figure 4-figure supplement 3a).

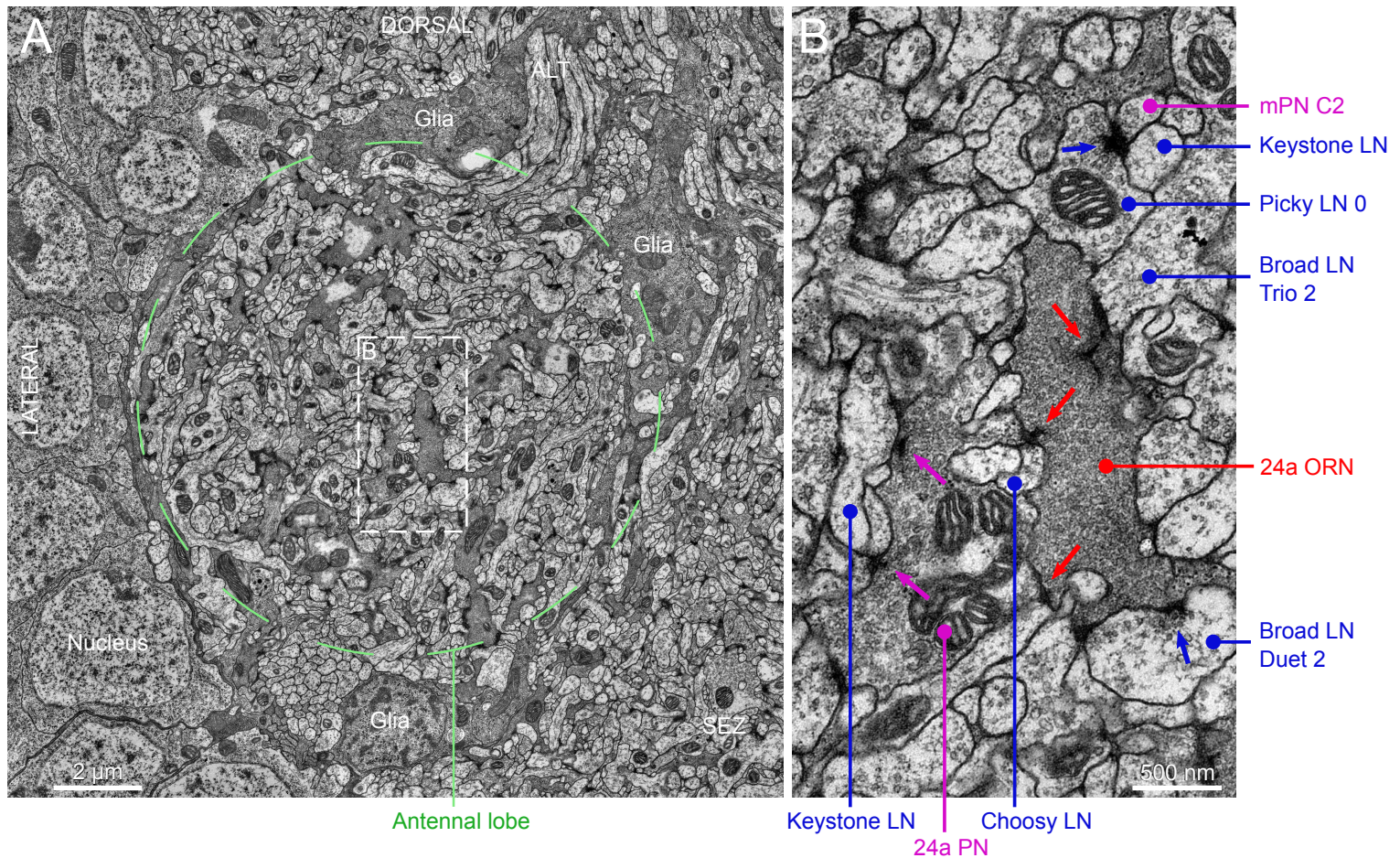
To determine which ORNs encode the regions of each cluster, we projected back the centroid of each cluster onto ORN space using the inverse transformation (Figure 4-figure supplement 3e). Different subsets of ORNs were more likely to encode each cluster. The projections of the cluster centroids in ORN space are not discrete numbers; in order to make these results easier to interpret a threshold can be established to determine

which ORNs encode a cluster centroid and which ones don't. A suitable approach is to use Otsu's method, which can be considered a one-dimensional discrete analog of Fisher's discriminant analysis [78]. We obtained a threshold of 0.4725, which we used to determine the ORNs that encode each cluster (dashed red line in Figure 4-figure supplement 3e).

In [37] a set of odorants that specifically activate single ORNs at low concentrations were identified. These data can easily be used to cross-validate the predicted receptive field of the different ORNs in our analysis. Four of the odorants tested were alcohols and activated Or13a, 35a, 67b and 85c all of which are in our alcohols group. Other three were aromatics and activated Or22c, 24a and 30a, which are all in our aromatics group. One was a pyrazine and activated Or33b which is in our pyrazine group. Finally pentyl acetate (an ester) activated 47a which is in our esters group. The other odorants in [37] were in regions of odor space (mostly ketones and aldehydes) that were not sampled in [35] or [36] and therefore their responses cannot be predicted with our analysis. As more datasets are collected, approaches like the one we present here can be used to better establish the receptive field of each ORN.

## Acknowledgements

We thank Ingrid Andrade, Anton Miroschnikow, Ilona Brueckmann, Ivan Larderet, Volker Hartenstein, Bruno Afonso and Philipp Schlegel for contributing 15.5% of all reconstructed arbor cable, and Gaetan Vignoud for assistance with the PCA. We thank Rachel Wilson, Kathy Nagel, Andreas Thum, Bertram Gerber, Markus Knaden, Marc Gershow, Mei Zhen and Ibrahim Tastekin for constructive comments and discussions. A.D.T.S. thanks "The Harvard Brain Initiative Collaborative Seed Grant Program", the NIH Pioneer Award (8DP1GM105383), NIH PO1 (1P01GM103770), NSF BRAIN Initiative (NSF- IOS-1556388) and Harvard Brain Initiative Collaborative Seed Grant. M.E.B. thanks the NSF Physics of Living Systems Student Network. M.L. and A.K. acknowledge support of the Spanish Ministry of Economy and Competitiveness, 'Centro de Excelencia Severo Ochoa 2013-2017', SEV-2012-0208 and grants MICINN BFU2011-26208. AK acknowledges the support of the 'la Caixa' International PhD programme. We thank the Fly EM Project Team at HHMI Janelia for the gift of the EM volume, the HHMI visa office, and HHMI Janelia for funding.





## Anterior glomeruli

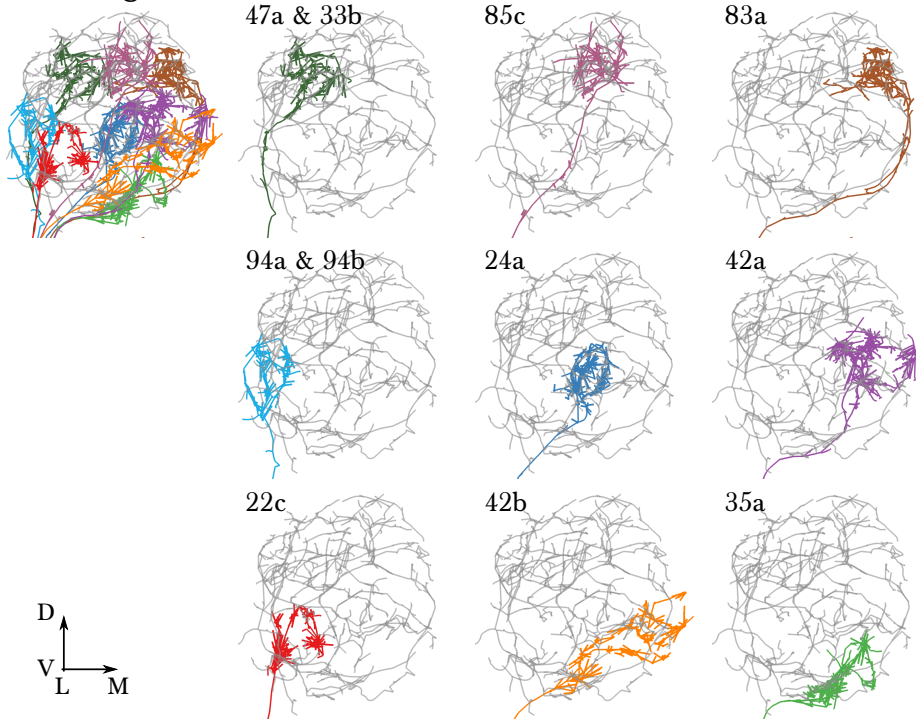
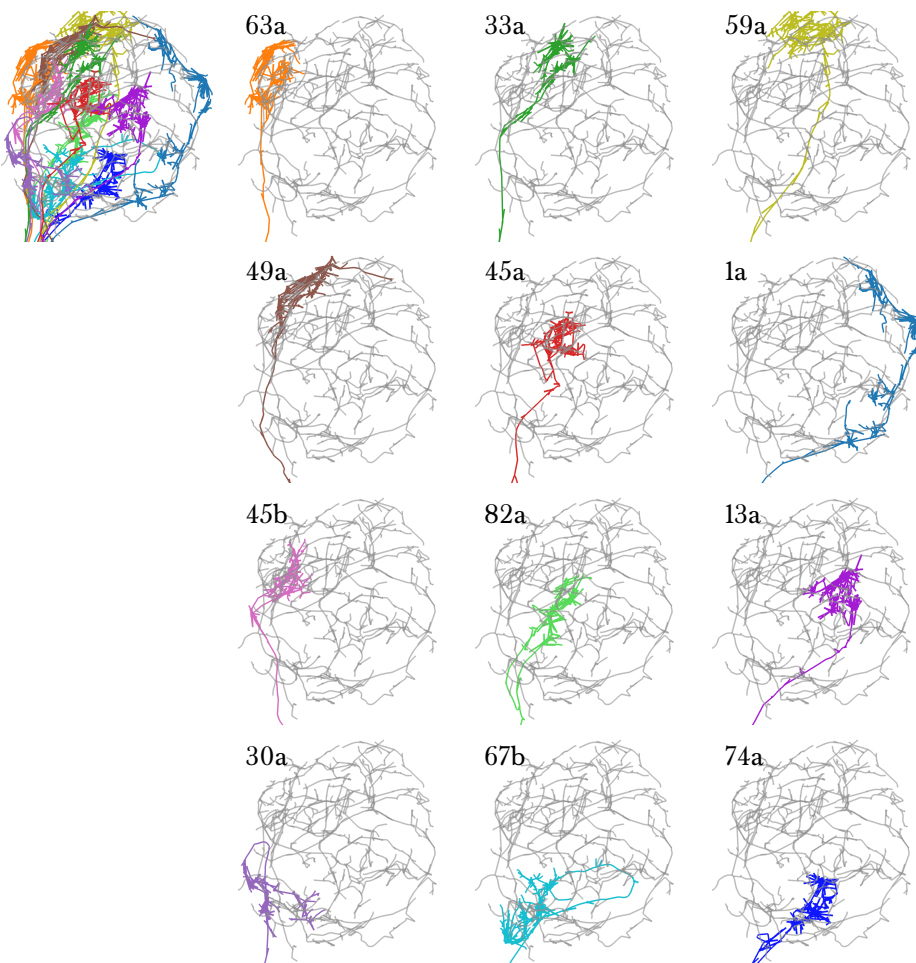


Figure 1-figure supplement 2: **A single, identified ORN for each glomerulus in the antennal lobe of the first instar larva.** Each panel shows an EM-reconstructed arbor of an ORN (colored) over the background of a Broad LN Duet (grey). ORN synapses are rendered in the same color as the skeleton. To the left, all ORNs of each half of the antennal lobe are rendered together. The orientation (lateral to the left, dorsal up) and relative position of each ORN has been chosen to exactly match the arrangement in the supplementary figure 1 of Masuda-Nakagawa et al. 2009, where each individual ORN was identified and labeled with GFP using genetic driver lines.

## Intermediate and posterior glomeruli



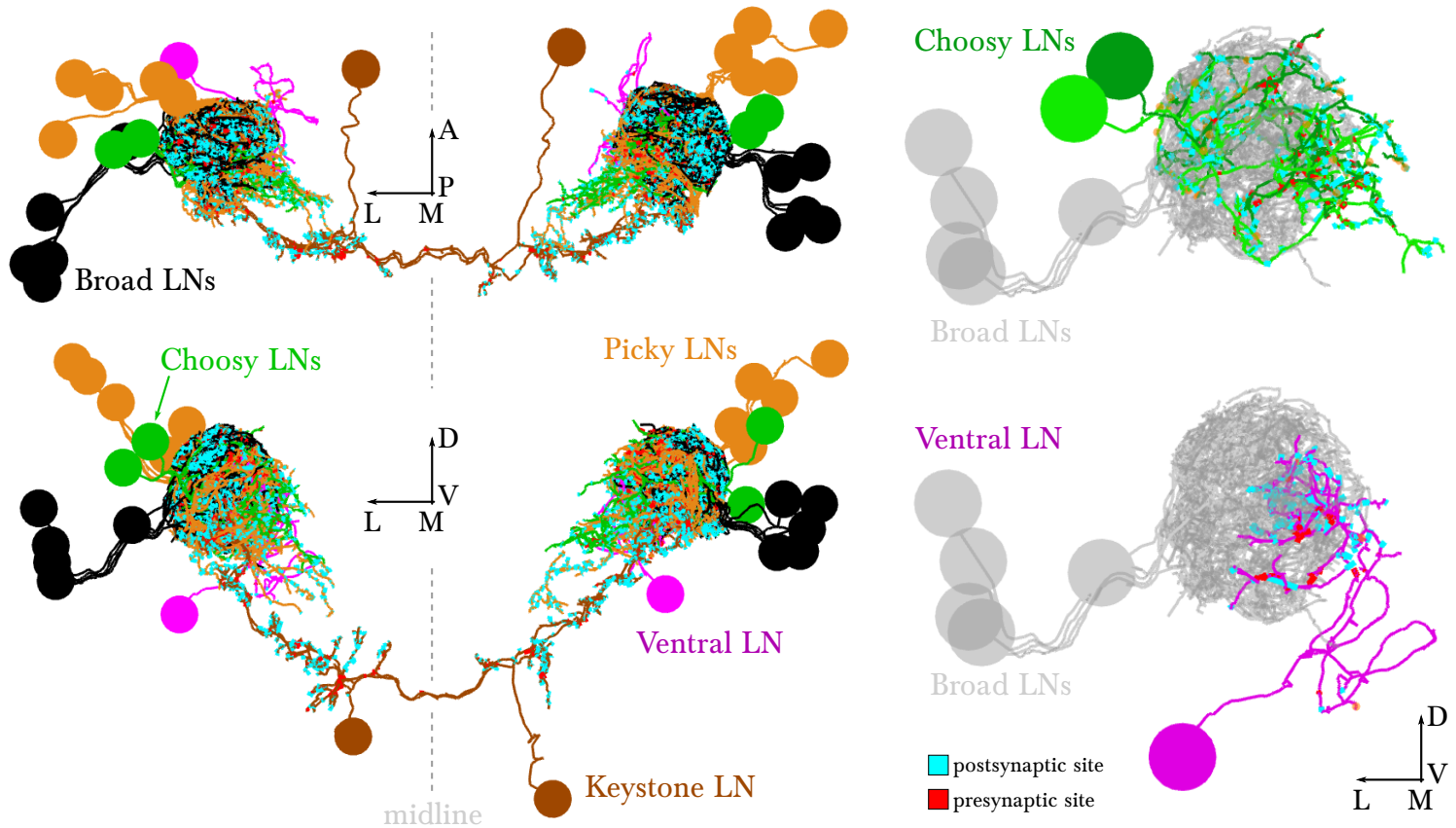
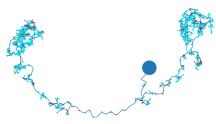


Figure 1-figure supplement 3: **EM-reconstructed arbors of all LNs.** *Left* dorsal and posterior views of all LNs. The bundling of their primary axon tracts suggests that all LNs derive from 5 neuronal lineages (5 on the left and 5 on the right), shown in 5 different colors. *Right*, renderings of the left antennal lobe, posterior view. These identified neurons present similar morphology and connectivity in the right antennal lobe. Broad LNs are shown for reference. The morphology, cell body position and number of Choosy LNs matches that of the pair of GABAergic LNs described in fig. 2 L-O of Thum et al., 2011. Scale bar: a cell body measures about 4 micrometers in diameter.

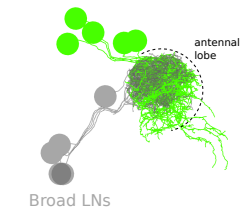


# EM-RECONSTRUCTIONS

## Keystone LN

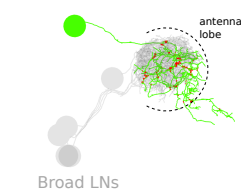


## Picky LNs



## Broad LNs

## Picky LN 4



## Broad LNs

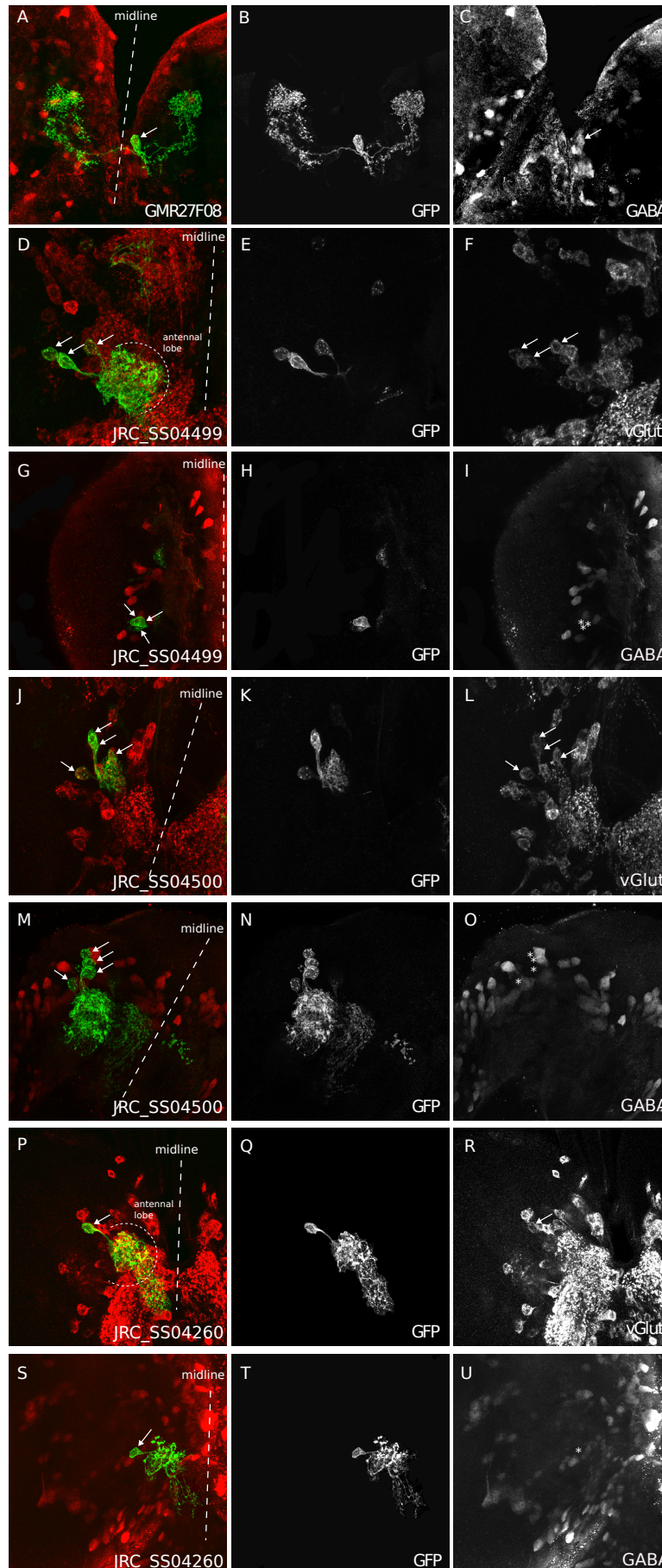


**Figure 2-figure supplement 1: Neurotransmitters of Keystone LN and Picky LNs.** Genetic driver lines specific for Keystone LN (GAL4 line GMR27F08) and Picky LNs (split-GAL4 lines JRC\_SS04499, JRC\_SS04500, JRC\_SS04260) driving GFP expression specifically in these neurons were labeled with anti-GABA and anti-vGlut (A-U), and also anti-Chat (all negative; not shown). Keystone presents immunoreactivity to anti-GABA (textbfA-C), and at least 4 of the 5 Picky LNs are positive to anti-vGlut and negative to anti-GABA (D-U). These neurons derive from the BAla2 lineage [19]. JRC\_SS04260 drives expression specifically and uniquely a Picky LN, likely Picky LN 4, which presents anti-vGlut immunoreactivity (P-R). *Left* unlettered panels show the homologous identified EM-reconstructed neurons, with Broad LNs in grey for reference. Asterisks mark the location of cell bodies when there is not labeling, such as in panels I, O and U. Broad LNs and Choosy LNs are GABAergic (see Thum et al., 2011 at fig. 2 D-G for Broad LNs and L-O for Choosy LNs).

Right Antennal Lobe		uPNs																				LNs														
		1a	13a	22c	24a	30a	33a	35a L	35a R	42a	42b	45a	45b	47a/33b	49a	59a	63a	67b	74a	82a	83a	85c	94a/94b	Broad LN Trio (3)	Broad LN Duet (2)	Keystone LN (2)	Choosy LN (2)	Ventral LN	Picky LN 0	Picky LN 1	Picky LN 2	Picky LN 3	Picky LN 4			
ORNs		1a	55																					1	3											
		13a		59																				3	4	2	7	29	2	7	3				16	3
		22c			48																			4	6	2	1		9	5	4					
		24a				48																		2	4	3		6	16	14						
		30a					69																	1	1	2						11			4	
		33a						66							2									1	1											
		35a							40	45										3				3	2	4							6	2		
		42a									50													3	3	4						16	18		1	
		42b										48												2	3	3					2	1		7	10	
		45a											58											2	1	2	2								9	
		45b												44										2	2		1									
		47a/33b													15	60								2	2											
		49a														46								2	4	1					5		9			
		59a															64							2	4		2	1								
	63a																49						3	5	1	1										
	67b																	53					2	5	2											
	74a																		62				2	5	4											
	82a																			34			1	2	2	6										
	83a																				62	8		1	1	1										
	85c																					47		3	5	1	1									
	94a/94b																						45		2	1	2	8								
																							44	65	38	28	35	64	62	53	39	42				
LNs	% ORN Input		55	59	54	48	69	69	40	45	51	48	61	61	65	46	64	52	53	65	40	62	55	45	44	65	38	28	35	64	62	53	39	42		
	Broad LN Trio (3)		3	6	10	11	3	6	5	10	5	6	2	11	4	7	8	9	10	8		7	7	13	14	6	12	6	7	4	7	4	8	3		
	Broad LN Duet (2)		24	16	20	18	15	9	2	2	9	15	17	20	20	34	18	30	18	14	13	13	27	14	2	3	1	5	3	9	5	4	4	2		
	Keystone LN (2)								2	1	10	11													5	1		5		2	6	4	1	2		
	Choosy LNs (2)								8	8	7	2	5												2		3			1	4	1		2		
	Ventral LN																								1	1	1	4								
	Picky LN 0																								1	1	8	2	4							
	Picky LN 1																																			
Desc. and Modulatory	Picky LN 2																																			
	Picky LN 3																																			
	Picky LN 4																																			
	% LN Input		27	39	38	43	22	15	18	28	39	39	31	31	24	47	31	42	37	29	37	34	42	39	22	16	22	32	17	19	31	27	15	18		
% ORN+LN Input		82	98	92	91	92	84	58	73	91	88	92	91	89	93	95	94	89	94	77	96	97	85	66	81	60	59	51	83	93	80	54	60			
	Descending CSD (2)																									1	3									
	IAL-1 (2)																									2	1									
	tdc (2)																									2										

Figure 3—figure supplement 1: **Extended version of table in fig. 3c, including all other olfactory-related neurons.** Tables show percent of post-synaptic sites of a column neuron contributed by a row neuron. We show only connections with at least two synapses, consistently found among homologous identified neurons in both the left and right antennal lobes. Percentages between 0 and 0.5 are removed. For bilateral neurons, inputs from both sides are included.

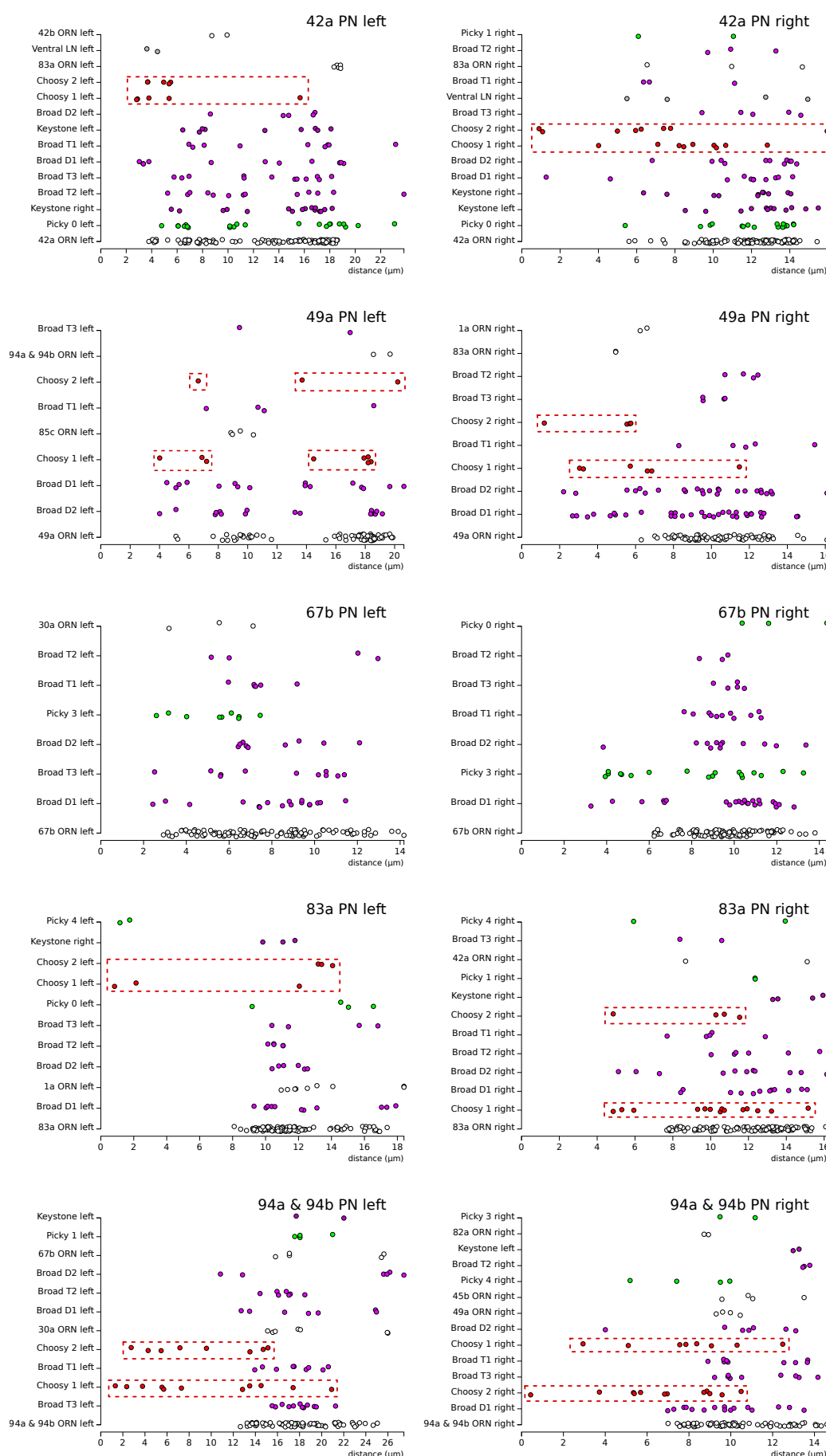
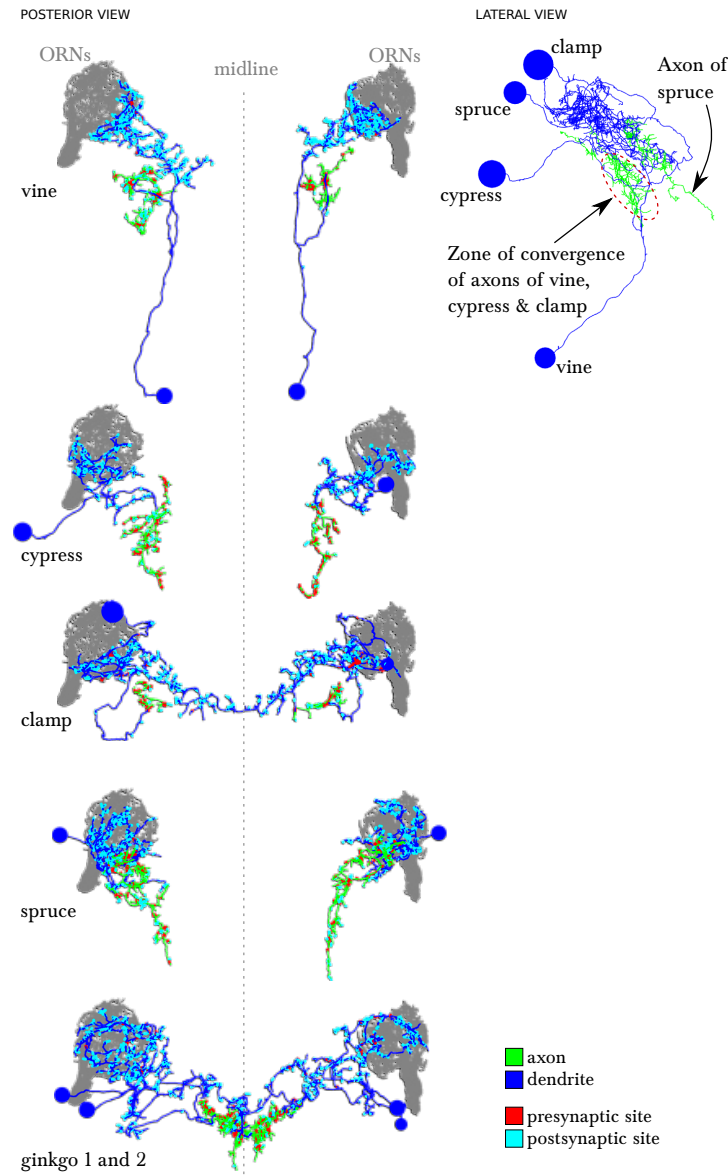


Figure 3—figure supplement 2: **Distribution of postsynaptic sites on the uPN dendrites.** We show 5 examples, plotting the distance (along the cable) of individual postsynaptic sites (colored dots) to the axon initial segment of each uPN. The same type of presynaptic neuron presents the same color across all plots. Notice how Choosy LN inputs (red, framed in a red box) onto uPNs are generally more proximal to the axon initial segment than other inhibitory inputs such as from Broad LNs; particularly noticeable for 42a PN (top row) and 94 & 94b PN (bottom row). No noticeable difference exists between Broad LN Duet and Trio. Notice that the left 49a PN presents an arbor with two main dendrites, with one being further than the other from the axon initial segment, explaining the split in the distribution of distances of postsynaptic sites. While 67b PN (third row) does not receive inputs from Choosy LNs, the Picky LN 3 (light green), which specifically targets 67b PN and no other uPN, provides proximal inputs. Presynaptic neurons are ordered with the largest contributor at the bottom of each plot.

# SEZ interneurons



Right antennal lobe		SEZ interneurons					
		vine	cypress	clamp	spruce	ginkgo 1	ginkgo 2
ORNs + uPNs	1a	4					
	13a						
	22c						
	24a						
	30a		14		6		
	33a						
	35a	12		3			
	42a						
	42b	11					
	45a					9	6
	45b						
	47a/33b				8		4
	49a						
	59a						
	63a						
	67b		8		8		
	74a						
	82a						
	83a						
	85c						
	94a/94b					1	
LNs	%ORN Input	27	22	3	24	9	10
	Broad LN trio (3)	4	2		1		
	Broad LN duet (2)	1					3
	Keystone LN (2)		2				
	Choosy LN (2)	7	1	2		9	
	Ventral LN			2			
	Picky LN 0						
	Picky LN 1						
Descending & modulatory	Picky LN 2	2					10
	Picky LN 3		12	2	12		4
	Picky LN 4	2				9	4
	%LN Input	17	16	5	14	18	20
Descending & modulatory	Descending CSD (2)						
	IAL-1 (2)	2					
	tdc (2)		3				

Figure 4—figure supplement 1: **Six SEZ neurons receive specific inputs from some ORNs and from some antennal lobe LNs.** *Left*, EM-reconstruction of the 6 SEZ neurons (vine, cypress, clamp, spruce and ginkgo 1 and 2), with their axons labeled green and their dendrites blue. Presynaptic sites in red and postsynaptic sites in cyan. *Middle*, 3 of these SEZ neurons project to the same unidentified region of the SEZ. Spruce projects to a more posterior area. Lateral view, anterior to the left. *Right*, table of percent of postsynaptic sites of a column neuron contributed by a row neuron, illustrating how some ORNs and LNs specifically target these SEZ neurons. We show only connections with at least two synapses, consistently found among homologous identified neurons in both the left and right antennal lobes. Percentages between 0 and 0.5 are removed. Notice how Picky LNs 2, 3 and 4 synapse strongly onto SEZ neurons.



Right Antennal Lobe		mPNs																	LNs									
		A1	A2	A3	B1	B2	B3	C1	C2	bil.-lower L	bil.-lower R	bil.-upper L	bil.-upper R	VUM L	VUM R	D	cobra	seahorse	Broad LN Trio (3)	Broad LN Duet (2)	Keystone LN (2)	Choosy LN (2)	Ventral LN	Picky LN 0	Picky LN 1	Picky LN 2	Picky LN 3	Picky LN 4
Glomeruli (ORN+uPN)	1a	1															11		1	3							16	3
	13a	3					1		1										4	4	3	7	34	2	8	3		
	22c			2						2	2						1		5	7	3	1		9	5	5		
	24a	3																	4	4	4	1	6	16	14			
	30a	6	2			11		4		2	3							2	2	2					11		5	
	33a			6			5			7	6	6	7					1	1									
	35a	2				14		4										3	2	4						6	2	
	42a	5													4	4		1	4	4	6			16	19		1	
	42b	6				1								3	3		7		4	3	5			2	1	7	13	
	45a	4				5	2			4	2	1	2				10		2	1	3	2				3	9	
	45b		2				4			4	5	1	2				1	1	3	3		1				5		
	47a/33b	5								7	11						20		3	5	1			5		9		
	49a	1	1			5	8			3	5								3	5		1						
	59a	3				10	5			2	1	1	1						3	4	2	1				2		
	63a	3								7	4						6		4	6	1	2				6		
	67b	5				7			1	2	4								4	6	2	3				4	4	
	74a	2			4	4		6	3									3	4	6	5					7	9	
	82a	1		8			1							3	6			16	1	2	2	6		6	6	4		
	83a	2	3															5	2	2	1			2	7			
	85c	6	4			1										11			5	5	2	2		9	3		2	
	94a/94b					4				9	9	1	1			6		31	3	1	3	9						
% ORN+uPN input		59	11	16	4	61	25	14	5	48	50	11	12	9	13	55	32	47	64	76	48	37	40	67	63	55	41	47
LNs	Broad LN Trio (3)	4	1	2		5	6	1	3	4	5	8	6			7	4	2	14	6	12	6	7	4	7	4	8	3
	Broad LN Duet (2)	2	1	2		1	3		7	2	2	22	22	8	6	4	2		2	3	1	5	3	9	5	4	4	2
	Keystone LN (2)				1	3				1	1			1	2	9	6		5	1		5		2	6	4	1	2
	Choosy LN (2)			4	3	6	2		1	1	1	4	8				1		2			3	1	1	4	1	2	
	Ventral LN				4	1											7		1	1	1	4		2	3	6	4	
	Picky LN 0	2		8				4						2	2		2	2	1	1	8	2	4		5	1	4	
	Picky LN 1	3		6			1			16	12	6	5	3	4			2		1	1	2						
	Picky LN 2		1	5			3			1	2	6	9	4	3	1	10					1			1			
	Picky LN 3	7				4																2						
Picky LN 4		25	4		3	17	1		3	3	4	4	2	8	6	12	3		1		3	4		1	7	2		
% LN Input		18	28	32	8	22	32	3	15	27	25	49	54	20	25	26	31	23	22	16	22	32	17	19	31	27	15	18
% ORN+uPN+LN input		77	39	48	12	84	57	17	20	75	75	61	66	29	38	81	63	69	87	92	70	69	57	86	94	82	56	65
Desc. and Modulatory	Descending		1	2			8	1		6	4	6	1	2	3		2					1			1	1		
	CSD (2)	2			5			1	5								1			1	3					1		
	IAL-1 (2)		2				1										2		2	1		1	5	2		3		
	tdc (2)					1		2				1	1	1	2				2							1		

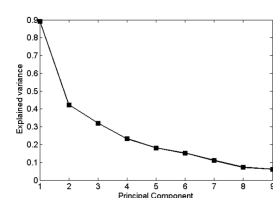
Figure 4—figure supplement 2: **Extended version of table in fig. 4c, including all other olfactory-related neurons.** Tables show percent of post-synaptic sites of a column neuron contributed by a row neuron. We show only connections with at least two synapses, consistently found among homologous identified neurons in both the left and right antennal lobes. Percentages between 0 and 0.5 are removed. For bilateral neurons, inputs from both sides are included.

a

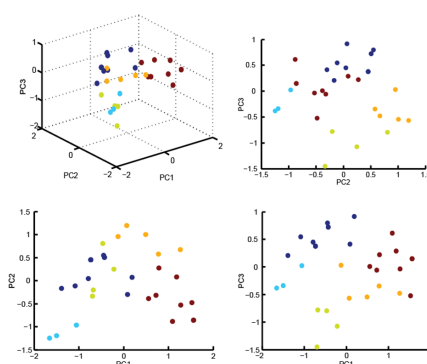
Cluster 1: Alcohols	Cluster 2: Esters	Cluster 3: Pyrazines	Cluster 4: Aromatics 1	Cluster 5: Aromatics 2
1-butanol 1-hexanol 1-octen-3-ol 1-heptanol 3-octanol 1-nonanol E2-hexenal 2-heptanone	Ethyl acetate Propyl acetate Pentyl acetate Isopentyl acetate Ethyl butyrate Geranyl acetate Propanoic acid Carbon dioxide	2-ethylpyrazine 2-methoxypyrazine 2,3-diethylpyrazine 2-isobutyl-3-methoxypyrazine 2,3-dimethylpyrazine 2,5-dimethylpyrazine Pyrazine	Methyl salicylate 2-methylphenol 4-methylphenol	Benzaldehyde Acetophenone Anisole Methyleugenol 2,3-butanedione cyclohexanone

The color code is Alcohols, Esters, Pyrazines, Aromatics, Others

b



c



d

Cluster 1: Alcohols	Cluster 2: Esters	Cluster 3: Pyrazines	Cluster 4: Aromatics	Cluster 5: Mixed
1-butanol 1-hexanol 1-octen-3-ol 1-heptanol 3-octanol E2-hexenal 2-heptanone cyclohexanone Pentyl acetate	Ethyl acetate Propyl acetate Isopentyl acetate Ethyl butyrate 2,3-butanedione	2-ethylpyrazine 2-methoxypyrazine 2,3-dimethylpyrazine 2,5-dimethylpyrazine	Benzaldehyde Acetophenone Anisole	1-nonanol Pyrazine 2,3-diethylpyrazine 2-isobutyl-3-methoxypyrazine Methyl salicylate 2-methylphenol 4-methylphenol Methyleugenol Geranyl acetate Propanoic acid Carbon dioxide

e

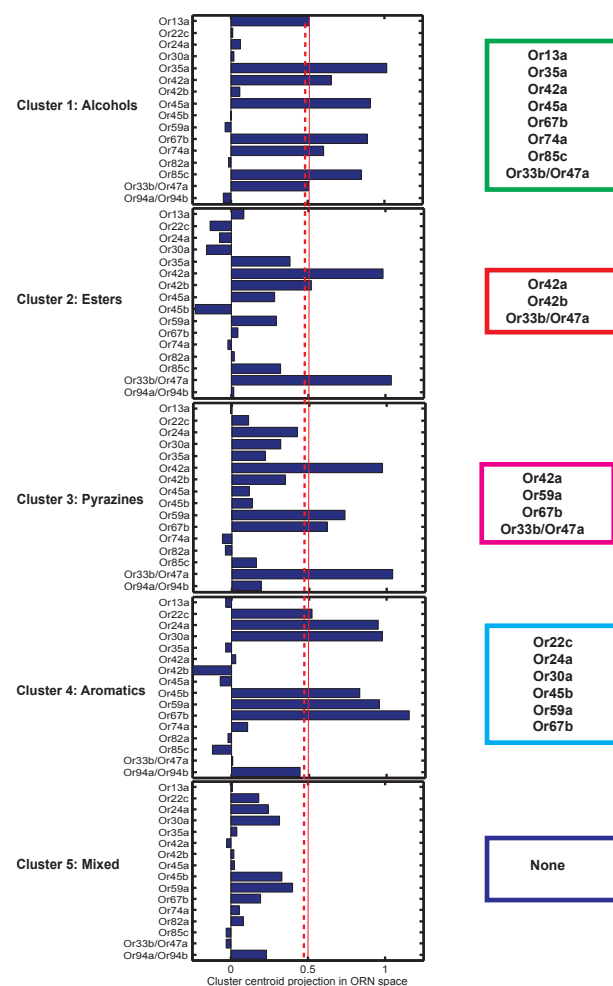
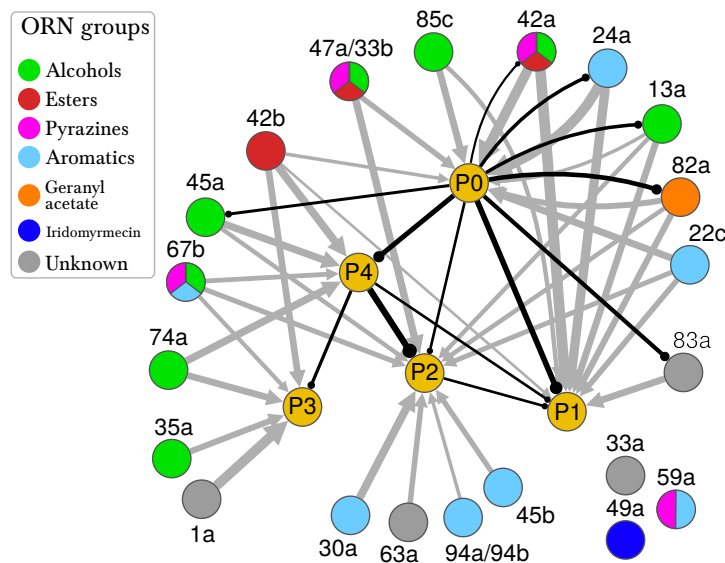


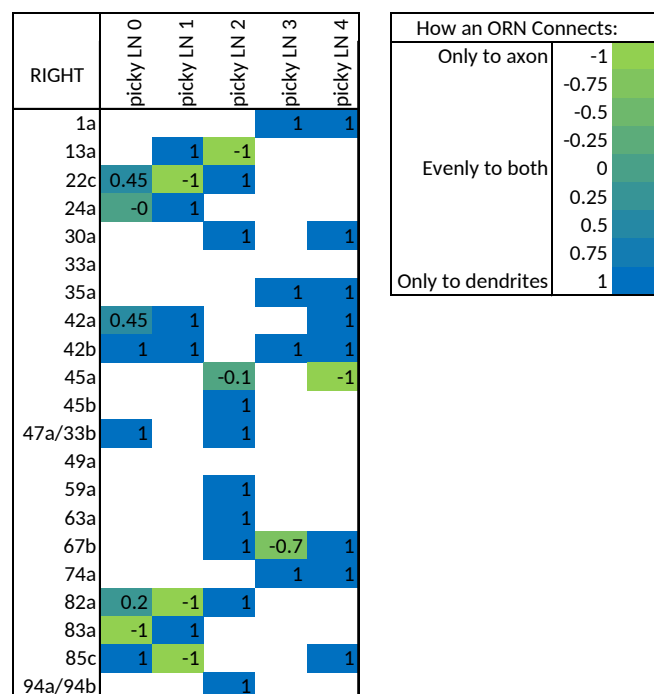
Figure 4—figure supplement 3: **Principal component analysis of odors leading to a principled clustering of ORNs.** **a** Clustering of odors by odorant-descriptor. Results of K-means clustering of odors in the 32 dimensional odor-descriptor space proposed in Haddad et al., 2008. Odors cluster into five groups that are well correlated with odor chemical type (alcohols, aromatics, esters, pyrazines, and others). **b-e** Clustering of odors by ORN response. **b** The variance explained for the odors in ORN response space as a function of the number of principal components (dimensions). The “elbow” of this curve is composed of the principal components used for the clustering analysis of the odors by ORN-response. **c** How the odors span the space of the first 3 principal components of ORN response space. The odors are individual points colored by which of the 5 clusters, calculated via an affinity propagation clustering algorithm, they belong to. **d** How each of the odors fit into the clusters in ORN response space. Each cluster tends to group odors of similar chemical type. **e** The ORNs that represent the centroid of each cluster, calculated using a threshold obtained via Otsu’s method. See materials and methods for further details.

## a ORN inputs onto Picky LNs



## b ORN inputs onto Picky LN axons or dendrites

(Inputs from ORN to Picky dend. - Inputs from ORN to Picky axon)  
(Inputs from ORN to Picky dend. + Inputs from ORN to Picky axon)



## c Picky LN hierarchy with axon/dendrite split

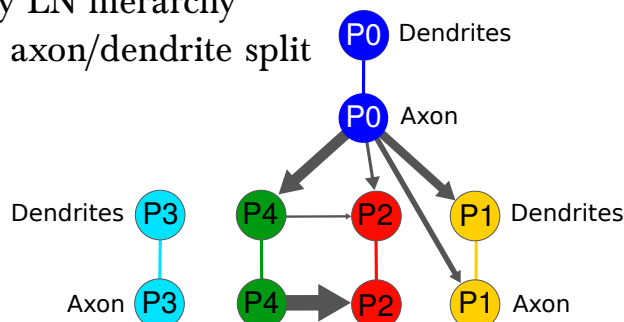


Figure 4—figure supplement 4: **Pattern of ORN inputs onto Picky LNs.** **A** The connections of ORNs onto the hierarchy of Picky LNs. ORNs are colored by the groups emerging from the PCA analysis of odor tuning. Inhibitory connections from Picky LNs are shown in black (only connections with 2 or more synapses among bilaterally homologous neuron pairs are shown). Excitatory connections from ORNs are shown in grey (only connections with 4 or more synapses among bilaterally homologous neuron pairs are shown). See Supplementary File 1 and 2 (containing the adjacency matrices) for the complete set of connections. The thickness of the arrows is proportional to the square root of the number of synapses. Some of these connections are axo-axonic (see C). **B** ORNs can synapse onto the Picky neurons at either their dendrites or their axons. This table shows values from -1 to 1 based on the written formula. Values between -1 and 0 correspond to the ORN synapsing more to the axon of the Picky LN than the dendrite, and values between 0 and 1 correspond to the ORN synapsing more to the dendrite of the Picky LN than the axon. Only consistent connections between ORNs and Picky dendrites or ORNs and Picky axons with a threshold of at least 2 consistent synapses per side are used to calculate these ratios. For values that are not 1 or -1, the value can differ from side to side. Because the threshold is lowered from that of A, more connections appear, but since we only consider connections consistent in how they connect to the Picky LNs (to dendrite or axon), some of the weakest connections also drop out compared to A. **C** The Picky LN hierarchy shown with the Picky LNs split into axon and dendrite, showing that not all connections are from the axon of a Picky LN to the dendrites of another. We are only showing connections that are consistent both in their motif (axo-axonic, dendro-dendritic, etc) and with a consistent threshold of 2 synapses on both sides. Because these criteria are more stringent than those used in A, some connections drop out (such as Picky LN 4 to Picky LN 3).

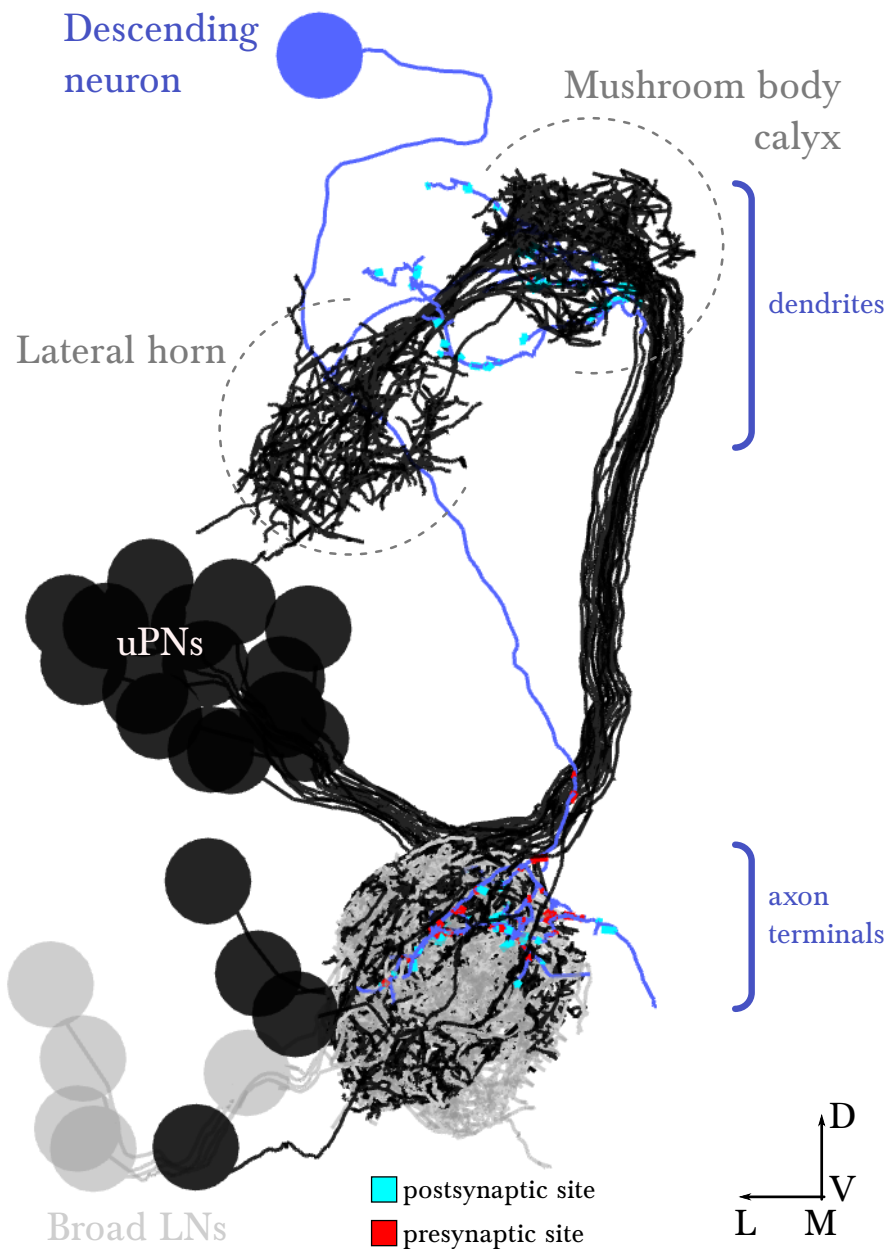


Figure 5–figure supplement 1: **EM-reconstructed arbor of the descending neuron.** Renderings of the left antennal lobe, posterior view. This identified neuron exists in the left and right antennal lobes, presenting similar morphology and connectivity in the right antennal lobe. Broad LNs and uPNs are shown for reference. Scale bar: a cell body measures about 4 micrometers in diameter.



Supplementary File 1 and 2: **Adjacency matrices with the complete synaptic connectivity of the wiring diagram.**

## References

- [1] Fan Wang, Adriana Nemes, Monica Mendelsohn, and Richard Axel. Odorant receptors govern the formation of a precise topographic map. *Cell*, 93(1):47–60, 1998.
- [2] Leslie B Vosshall, Allan M Wong, and Richard Axel. An olfactory sensory map in the fly brain. *Cell*, 102(2):147–159, 2000.
- [3] RF Stocker, MC Lienhard, A Borst, and KF Fischbach. Neuronal architecture of the antennal lobe in *Drosophila melanogaster*. *Cell and Tissue Research*, 262(1):9–34, 1990.
- [4] Liang Liang, Yulong Li, Christopher J Potter, Ofer Yizhar, Karl Deisseroth, Richard W Tsien, and Liqun Luo. Gabaergic projection neurons route selective olfactory inputs to specific higher-order neurons. *Neuron*, 79(5):917–931, 2013.
- [5] LB Vosshall and RF Stocker. Molecular architecture of smell and taste in *Drosophila*. *Annu Rev Neurosci*, 30:505–33, 2007.
- [6] Chih-Ying Su, Karen Menuz, and John R Carlson. Olfactory perception: receptors, cells, and circuits. *Cell*, 139(1):45–59, 2009.
- [7] KF Fischbach and M Heisenberg. Neurogenetics and behaviour in insects. *Journal of Experimental Biology*, 112(1):65–93, 1984.
- [8] Martin Heisenberg, Alexander Borst, Sibylle Wagner, and Duncan Byers. *Drosophila* mushroom body mutants are deficient in olfactory learning: Research papers. *Journal of Neurogenetics*, 2(1):1–30, 1985.
- [9] Dara L Sosulski, Maria Lissitsyna Bloom, Tyler Cutforth, Richard Axel, and Sandeep Robert Datta. Distinct representations of olfactory information in different cortical centres. *Nature*, 472(7342):213–216, 2011.
- [10] Shawn R Olsen and Rachel I Wilson. Lateral presynaptic inhibition mediates gain control in an olfactory circuit. *Nature*, 452(7190):956–960, April 2008.
- [11] J Rybak, G Talarico, S Ruiz, C Arnold, R Cantera, and BS Hansson. Synaptic circuitry of identified neurons in the antennal lobe of *Drosophila melanogaster*. *The Journal of comparative neurology*, 2016.
- [12] Elane Fishilevich, Ana I Domingos, Kenta Asahina, Félix Naef, Leslie B Vosshall, and Matthieu Louis. Chemotaxis behavior mediated by single larval olfactory neurons in *Drosophila*. *Current Biology*, 15(23):2086–2096, 2005.
- [13] Liria M Masuda-Nakagawa, Nanaë Gendre, Cahir J O’Kane, and Reinhard F Stocker. Localized olfactory representation in mushroom bodies of *Drosophila* larvae. *Proceedings of the National Academy of Sciences USA*, 106(25):10314–10319, 2009.
- [14] Laurina Manning, Ellie S Heckscher, Maria D Purice, Jourdain Roberts, Alysha L Bennett, Jason R Kroll, Jill L Pollard, Marie E Strader, Josh R Lupton, Anna V Dyukareva, et al. A resource for manipulating gene expression and analyzing cis-regulatory modules in the *Drosophila* CNS. *Cell Reports*, 2(4):1002–1013, 2012.
- [15] Joshua T Vogelstein, Youngser Park, Tomoko Ohyama, Rex A Kerr, James W Truman, Carey E Priebe, and Marta Zlatić. Discovery of brainwide neural-behavioral maps via multiscale unsupervised structure learning. *Science*, 344(6182):386–392, 2014.
- [16] H.-H. Li, J. R. Kroll, S. M. Lennox, O. Ogundeyi, J. Jeter, G. Depasquale, and J. W. Truman. A GAL4 Driver Resource for Developmental and Behavioral Studies on the Larval CNS of *Drosophila*. *Cell Reports*, 8(3):897–908, 2014.
- [17] Tomoko Ohyama, Casey M Schneider-Mizell, Richard D Fetter, Javier Valdes Aleman, Romain Franconville, Marta Rivera-Alba, Brett D Mensh, Kristin M Branson, Julie H Simpson, James W Truman, Albert Cardona, and Marta Zlatić. A multilevel multimodal circuit enhances action selection in *Drosophila*. *Nature*, 520:633–39, 2015.
- [18] Andreas Stephan Thum, Basil Leisibach, Nanae Gendre, Mareike Selcho, and Reinhard F Stocker. Diversity, variability, and suboesophageal connectivity of antennal lobe neurons in d. melanogaster larvae. *Journal of Comparative Neurology*, 519(17):3415–3432, 2011.
- [19] Abhijit Das, Tripti Gupta, Sejal Davla, Lucia L Prieto-Godino, Sören Diegelmann, O Venkateswara Reddy, K Vijay Raghavan, Heinrich Reichert, Jennifer Lovick, and Volker Hartenstein. Neuroblast lineage-specific origin of the neurons of the *Drosophila* larval olfactory system. *Developmental biology*, 373(2):322–337, 2013.
- [20] Rainer W Friedrich and Sigrun I Korsching. Combinatorial and chemotopic odorant coding in the zebrafish olfactory bulb visualized by optical imaging. *Neuron*, 18(5):737–752, 1997.

- [21] Shin Nagayama, Yuji K Takahashi, Yoshihiro Yoshihara, and Kensaku Mori. Mitral and tufted cells differ in the decoding manner of odor maps in the rat olfactory bulb. *Journal of Neurophysiology*, 91(6):2532–2540, 2004.
- [22] Vikas Bhandawat, Shawn R Olsen, Nathan W Gouwens, Michelle L Schlieff, and Rachel I Wilson. Sensory processing in the *Drosophila* antennal lobe increases reliability and separability of ensemble odor representations. *Nature Neuroscience*, 10(11):1474–1482, 2007.
- [23] Katherine I Nagel and Rachel I Wilson. Biophysical mechanisms underlying olfactory receptor neuron dynamics. *Nature neuroscience*, 14(2):208–216, 2011.
- [24] Anmo J Kim, Aurel A Lazar, and Yevgeniy B Slutskiy. Projection neurons in *Drosophila* antennal lobes signal the acceleration of odor concentrations. *eLife*, page e06651, 2015.
- [25] Kenta Asahina, Matthieu Louis, Silvia Piccinotti, and Leslie B Vosshall. A circuit supporting concentration-invariant odor perception in *Drosophila*. *Journal of Biology*, 8(1):9, 2009.
- [26] Aljoscha Schulze, Alex Gomez-Marin, Vani G Rajendran, Gus Lott, Marco Musy, Parvez Ahammad, Ajinkya Deogade, James Sharpe, Julia Riedl, David Jarriault, et al. Dynamical feature extraction at the sensory periphery guides chemotaxis. *eLife*, 4:e06694, 2015.
- [27] Peixin Zhu, Thomas Frank, and Rainer W Friedrich. Equalization of odor representations by a network of electrically coupled inhibitory interneurons. *Nature Neuroscience*, 16(11):1678–1686, 2013.
- [28] Matthew Cobb. What and how do maggots smell? *Biological reviews*, 74(4):425–459, 1999.
- [29] Dennis Bellmann, Arnd Richardt, Robert Freyberger, Nidhi Nuwal, Martin Schwärzel, André Fiala, and Klemens F Störtkuhl. Optogenetically induced olfactory stimulation in *Drosophila* larvae reveals the neuronal basis of odor-aversion behavior. *Frontiers in Behavioral Neuroscience*, 4, 2010.
- [30] Alex Gomez-Marin, Greg J Stephens, and Matthieu Louis. Active sampling and decision making in *Drosophila* chemotaxis. *Nature Communications*, 2:441, 2011.
- [31] Marc Gershow, Matthew Berck, Dennis Mathew, Linjiao Luo, Elizabeth A Kane, John R Carlson, and Aravinthan DT Samuel. Controlling airborne cues to study small animal navigation. *Nature Methods*, 9(3):290–296, 2012.
- [32] Ruben Gepner, Mirna Mihovilovic Skanata, Natalie M Bernat, Margarita Kaplow, and Marc Gershow. Computations underlying *Drosophila* photo-taxis, odor-taxis, and multi-sensory integration. *eLife*, page e06229, 2015.
- [33] Luis Hernandez-Nunez, Jonas Belina, Mason Klein, Guangwei Si, Lindsey Claus, John R Carlson, and Aravinthan DT Samuel. Reverse-correlation analysis of navigation dynamics in *Drosophila* larva using optogenetics. *eLife*, page e06225, 2015.
- [34] M Louis, T Huber, R Benton, TP Sakmar, and LB Vosshall. Bilateral olfactory sensory input enhances chemotaxis behavior. *Nature Neuroscience*, 11(2):187–99, 2008.
- [35] Scott A Kreher, Dennis Mathew, Junhyong Kim, and John R Carlson. Translation of sensory input into behavioral output via an olfactory system. *Neuron*, 59(1):110–124, 2008.
- [36] Shelby A Montague, Dennis Mathew, and John R Carlson. Similar odorants elicit different behavioral and physiological responses, some supersustained. *The Journal of Neuroscience*, 31(21):7891–7899, 2011.
- [37] Dennis Mathew, Carlotta Martelli, Elizabeth Kelley-Swift, Christopher Brusalis, Marc Gershow, Aravinthan DT Samuel, Thierry Emonet, and John R Carlson. Functional diversity among sensory receptors in a *Drosophila* olfactory circuit. *Proceedings of the National Academy of Sciences USA*, 110(23):E2134–E2143, 2013.
- [38] Bertram Gerber. The *Drosophila* larva as a model for studying chemosensation and chemosensory learning: a review. *Chemical Senses*, 32(1):65–89, 2007.
- [39] F. Python and R.F. Stocker. Adult-like complexity of the larval antennal lobe of *Dr. melanogaster* despite markedly low numbers of odorant receptor neurons. *Cell Tissue Res*, 445(4):374–87, 2002.
- [40] S Saalfeld, A Cardona, V Hartenstein, and P Tomancak. CATMAID: Collaborative Annotation Toolkit for Massive Amounts of Image Data. *Bioinformatics*, 25(19):1984–1986, 2009.



- [41] Casey M Schneider-Mizell, Stephan Gerhard, Mark Longair, Tom Kazimiers, Feng Li, Maarten F Zwart, Andrew Champion, Frank M Midgley, Richard D Fetter, Stephan Saalfeld, and Albert Cardona. Quantitative neuroanatomy for connectomics in *Drosophila*. *eLife*, 5:e12059, mar 2016.
- [42] Mareike Selcho, Dennis Pauls, Annina Huser, Reinhard F Stocker, and Andreas S Thum. Characterization of the octopaminergic and tyraminergetic neurons in the central brain of *Drosophila* larvae. *Journal of Comparative Neurology*, 522(15):3485–3500, 2014.
- [43] Bidisha Roy, Ajeet P Singh, Chetak Shetty, Varun Chaudhary, Annemarie North, Matthias Landgraf, K Vijayraghavan, and Veronica Rodrigues. Metamorphosis of an identified serotonergic neuron in the *Drosophila* olfactory system. *Neural Dev*, 2:20, 2007.
- [44] Masahiko Satou. Synaptic organization of the olfactory bulb and its central projection. In Toshiaki J. Hara, editor, *Fish Chemoreception*, volume 6 of *Fish & Fisheries Series*, pages 40–59. Springer, 1992.
- [45] Kerry J Ressler, Susan L Sullivan, and Linda B Buck. Information coding in the olfactory system: evidence for a stereotyped and highly organized epitope map in the olfactory bulb. *Cell*, 79(7):1245–1255, 1994.
- [46] Paul G Distler and Jürgen Boeckh. Synaptic connection between olfactory receptor cells and uniglomerular projection neurons in the antennal lobe of the american cockroach, *periplaneta americana*. *Journal of Comparative Neurology*, 370(1):35–46, 1996.
- [47] A Ramaekers, E Magenat, EC Marin, N Gendre, GSXE Jefferis, L Luo, and RF Stocker. Glomerular Maps without Cellular Redundancy at Successive Levels of the *Drosophila* Larval Olfactory Circuit. *Current Biology*, 15(11):982–92, 2005.
- [48] Sean X Luo, Richard Axel, and LF Abbott. Generating sparse and selective third-order responses in the olfactory system of the fly. *Proceedings of the National Academy of Sciences USA*, 107(23):10713–10718, 2010.
- [49] Birgit Michels, Yi-chun Chen, Timo Saumweber, Dushyant Mishra, Hiromu Tanimoto, Benjamin Schmid, Olivia Engmann, and Bertram Gerber. Cellular site and molecular mode of synapsin action in associative learning. *Learning & Memory*, 18(5):332–344, 2011.
- [50] J Steven de Belle and Martin Heisenberg. Associative odor learning in drosophila abolished by chemical ablation of mushroom bodies. *Science*, 263(5147):692–695, 1994.
- [51] Silke Sachse and C Giovanni Galizia. Role of inhibition for temporal and spatial odor representation in olfactory output neurons: a calcium imaging study. *Journal of neurophysiology*, 87(2):1106–1117, 2002.
- [52] Hong Lei, Thomas A Christensen, and John G Hildebrand. Local inhibition modulates odor-evoked synchronization of glomerulus-specific output neurons. *Nature neuroscience*, 5(6):557–565, 2002.
- [53] Shawn R Olsen, Vikas Bhandawat, and Rachel I Wilson. Divisive normalization in olfactory population codes. *Neuron*, 66(2):287–299, 2010.
- [54] RI Wilson and G Laurent. Role of GABAergic inhibition in shaping odor-evoked spatiotemporal patterns in *Drosophila* antennal lobe. *J Neurosci*, 25:9069–79, 2005.
- [55] Ya-Hui Chou, Maria L Spletter, Emre Yaksi, Jonathan CS Leong, Rachel I Wilson, and Liqun Luo. Diversity and wiring variability of olfactory local interneurons in the *Drosophila* antennal lobe. *Nature Neuroscience*, 13(4):439–449, 2010.
- [56] Katherine I Nagel, Elizabeth J Hong, and Rachel I Wilson. Synaptic and circuit mechanisms promoting broadband transmission of olfactory stimulus dynamics. *Nature Neuroscience*, 18(1):56–65, 2015.
- [57] Wilfrid Rall, GM Shepherd, TS Reese, and MW Brightman. Dendrodendritic synaptic pathway for inhibition in the olfactory bulb. *Experimental Neurology*, 14(1):44–56, 1966.
- [58] Ryuichi Okada, Takeshi Awasaki, and Kei Ito. Gamma-aminobutyric acid (gaba)-mediated neural connections in the *Drosophila* antennal lobe. *Journal of Comparative Neurology*, 514(1):74–91, 2009.
- [59] Nathan W Gouwens and Rachel I Wilson. Signal propagation in *Drosophila* central neurons. *The Journal of Neuroscience*, 29(19):6239–6249, 2009.
- [60] Wendy W Liu and Rachel I Wilson. Glutamate is an inhibitory neurotransmitter in the *Drosophila* olfactory system. *Proceedings of the National Academy of Sciences USA*, 110(25):10294–10299, 2013.

- [61] Uri Alon. Network motif: theory and experimental approaches. *Nature Reviews Genetics*, 8(6):450–61, 2007.
- [62] SA Ebrahim, HK Dweck, J Stökl, JE Hofferberth, F Trona, K Weniger, J Rybak, Y Seki, MC Stensmyr, S Sachse, et al. *Drosophila* avoids parasitoids by sensing their semiochemicals via a dedicated olfactory circuit. *PLoS biology*, 13(12):e1002318, 2015.
- [63] Christiane Linster and Brian H Smith. A computational model of the response of honey bee antennal lobe circuitry to odor mixtures: overshadowing, blocking and unblocking can arise from lateral inhibition. *Behavioural brain research*, 87(1):1–14, 1997.
- [64] Andrew M Dacks, David S Green, Cory M Root, Alan J Nighorn, and Jing W Wang. Serotonin modulates olfactory processing in the antennal lobe of *Drosophila*. *Journal of Neurogenetics*, 23(4):366–377, 2009.
- [65] Mareike Selcho, Dennis Pauls, Basil el Jundi, Reinhard F Stocker, and Andreas S Thum. The role of octopamine and tyramine in *Drosophila* larval locomotion. *Journal of Comparative Neurology*, 520(16):3764–3785, 2012.
- [66] Xiaojing J Gao, Thomas R Clandinin, and Liqun Luo. Extremely sparse olfactory inputs are sufficient to mediate innate aversion in *Drosophila*. *PLoS ONE*, 10(4):e0125986, 2015.
- [67] Ramani Balu, R Todd Pressler, and Ben W Strowbridge. Multiple modes of synaptic excitation of olfactory bulb granule cells. *The Journal of Neuroscience*, 27(21):5621–5632, 2007.
- [68] Lucia L Prieto-Godino, Soeren Diegelmann, and Michael Bate. Embryonic origin of olfactory circuitry in *Drosophila*: contact and activity-mediated interactions pattern connectivity in the antennal lobe. *PLoS Biology*, 10(10):e1001400, 2012.
- [69] E Yaksi and RI Wilson. Electrical coupling between olfactory glomeruli. *Neuron*, 67:1034–47, 2010.
- [70] AM Wong, JW Wang, and R Axel. Spatial Representation of the Glomerular Map in the *Drosophila* Protocerebrum. *Cell*, 109:229–41, 2002.
- [71] Mehmet Fişek and Rachel I Wilson. Stereotyped connectivity and computations in higher-order olfactory neurons. *Nature Neuroscience*, 17(2):280–288, 2014.
- [72] Matteo Carandini. From circuits to behavior: a bridge too far? *Nature Neuroscience*, 15(4):507–509, 2012.
- [73] Daria Drobysheva, Kristen Ameel, Brandon Welch, Esther Ellison, Khan Chaichana, Bryan Hoang, Shilpy Sharma, Wendi Neckameyer, Irina Srinakevitch, Kelley J Murphy, et al. An optimized method for histological detection of dopaminergic neurons in *Drosophila melanogaster*. *Journal of Histochemistry & Cytochemistry*, 56(12):1049–1063, 2008.
- [74] Aljoscha Nern, Barret D Pfeiffer, and Gerald M Rubin. Optimized tools for multicolor stochastic labeling reveal diverse stereotyped cell arrangements in the fly visual system. *Proceedings of the National Academy of Sciences USA*, page 201506763, 2015.
- [75] Richard W Daniels, Catherine A Collins, Maria V Gelfand, Jaime Dant, Elizabeth S Brooks, David E Krantz, and Aaron DiAntonio. Increased expression of the *Drosophila* vesicular glutamate transporter leads to excess glutamate release and a compensatory decrease in quantal content. *The Journal of Neuroscience*, 24(46):10466–10474, 2004.
- [76] Rafi Haddad, Tali Weiss, Rehan Khan, Boaz Nadler, Nathalie Mandairon, Moustafa Bensafi, Elad Schneidman, and Noam Sobel. Global features of neural activity in the olfactory system form a parallel code that predicts olfactory behavior and perception. *The Journal of Neuroscience*, 30(27):9017–9026, 2010.
- [77] Rafi Haddad, Rehan Khan, Yuji K Takahashi, Kensaku Mori, David Harel, and Noam Sobel. A metric for odorant comparison. *Nature Methods*, 5(5):425–429, 2008.
- [78] Nobuyuki Otsu. A threshold selection method from gray-level histograms. *Automatica*, 11(285-296):23–27, 1975.
- [79] Lynne A. Oland, John P. Biebelhausen, and Leslie P. Tolbert. Glial investment of the adult and developing antennal lobe of *Drosophila*. *The Journal of comparative neurology*, (509):526–50, 2008.